

MODELLING THE AIRBORNE ELECTROMAGNETIC RESPONSE OF A SPHERE
UNDERLYING A UNIFORM CONDUCTIVE OVERBURDEN

by

Anthony Zamperoni

A thesis submitted in partial fulfillment
of the requirements for the degree of
Master of Science (MSc) in Geology

The Faculty of Graduate Studies
Laurentian University
Sudbury, Ontario, Canada

© Anthony Zamperoni, 2020

THESIS DEFENCE COMMITTEE/COMITÉ DE SOUTENANCE DE THÈSE
Laurentian Université/Université Laurentienne
Faculty of Graduate Studies/Faculté des études supérieures

Title of Thesis Titre de la thèse	MODELLING THE AIRBORNE ELECTROMAGNETIC RESPONSE OF A SPHERE UNDERLYING A UNIFORM CONDUCTIVE OVERBURDEN		
Name of Candidate Nom du candidat	Zamperoni, Anthony Daniel		
Degree Diplôme	Master of Science		
Department/Program Département/Programme	Geology	Date of Defence Date de la soutenance	May 15, 2020

APPROVED/APPROUVÉ

Thesis Examiners/Examineurs de thèse:

Dr. Richard Smith
(Supervisor/Directeur(trice) de thèse)

Mr. Warren Hughes
(Committee member/Membre du comité)

Dr. Mostafa Naghizadeh
(Committee member/Membre du comité)

Dr. Martyn Unsworth
(External Examiner/Examineur externe)

Approved for the Faculty of Graduate Studies
Approuvé pour la Faculté des études supérieures
Dr. David Lesbarrères
Monsieur David Lesbarrères
Dean, Faculty of Graduate Studies
Doyen, Faculté des études supérieures

ACCESSIBILITY CLAUSE AND PERMISSION TO USE

I, **Anthony Daniel Zamperoni**, hereby grant to Laurentian University and/or its agents the non-exclusive license to archive and make accessible my thesis, dissertation, or project report in whole or in part in all forms of media, now or for the duration of my copyright ownership. I retain all other ownership rights to the copyright of the thesis, dissertation or project report. I also reserve the right to use in future works (such as articles or books) all or part of this thesis, dissertation, or project report. I further agree that permission for copying of this thesis in any manner, in whole or in part, for scholarly purposes may be granted by the professor or professors who supervised my thesis work or, in their absence, by the Head of the Department in which my thesis work was done. It is understood that any copying or publication or use of this thesis or parts thereof for financial gain shall not be allowed without my written permission. It is also understood that this copy is being made available in this form by the authority of the copyright owner solely for the purpose of private study and research and may not be copied or reproduced except as permitted by the copyright laws without written authority from the copyright owner.

MODELLING THE AIRBORNE ELECTROMAGNETIC RESPONSE OF A SPHERE
UNDERLYING A UNIFORM CONDUCTIVE OVERBURDEN

by

Anthony Zamperoni

A thesis submitted in partial fulfillment
of the requirements for the degree of
Master of Science (MSc) in Geology

The Faculty of Graduate Studies
Laurentian University
Sudbury, Ontario, Canada

© Anthony Zamperoni, 2020

Abstract

Electromagnetic geophysical methods are used in mineral exploration to detect conductors at depth. In igneous and metamorphic settings, the background half-space is often largely resistive. In such cases, it is important to consider the interaction between the target conductor and any thin, conductive overburden that might exist above the half-space. The overburden is often comprised of glacial tills and clays or the weathering of basement rocks to more conductive material. This situation can be approximated using a discrete conductor model consisting of a “dipping sphere” in a resistive half-space underlying a uniform conductive overburden. A semi-analytical solution that considers the first-order interaction of the sphere and overburden has been derived to calculate the electromagnetic response. The simplicity and efficiency of this solution makes it well suited to be implemented when computation time and immediacy of results are desirable. To this end, we have developed a graphical user interface (GUI) based program to model the electromagnetic response of this model. The program allows users to change the parameters of the survey and target body and quickly view the resulting changes in the shape and decay of the electromagnetic response. The program was tested on airborne electromagnetic data from the Forrestania test range in western Australia. The sphere-overburden model as implemented in the program was able to fit the anomalous data with a spherical body buried 156 m deep and having a dip of 35 degrees to the north.

Keywords

Geophysics, airborne electromagnetic, forward model, program

Acknowledgments

Thank you to my supervisor Richard Smith for giving me this opportunity, thank you to all of my friends, family and fellow grad students that helped me over the course of the last couple of years. Thank you to Adam Smiarowski from CGG for providing the geophysical data used in this thesis.

Table of Contents

Thesis committee	ii
Abstract	iii
Acknowledgments.....	iv
Table of Contents.....	v
List of Tables	vii
List of Figures	viii
Chapter 1	1
1 Electromagnetic geophysics methods.....	1
1.1 EM geophysics theory	2
1.2 Discrete conductor models.....	5
1.3 Research goals.....	6
Chapter 2	8
2 Sphere-Overburden algorithm.....	8
Chapter 3	11
3 Program design.....	11
3.1 Program development.....	14
Chapter 4	15
4 Methods	15
4.1 Synthetic models	16
4.2 Modelling field data	19
4.3 Forrestania test site.....	19
4.4 HELITEM® data.....	21

Chapter 5	24
5 Forrestania modelling results	24
5.1 Comparison to Maxwell model	27
Chapter 6	29
6 Discussion and future work	29
6.1 Conclusions	30
References	32

List of Tables

Table 1: Time windows (in ms) used for the HELITEM® system when acquiring the Forrestania data.....	23
---	----

Table 2: Model parameters used in the modelling of the IR2 conductor response at the Forrestania EM test range using the sphere-overburden program.....	26
---	----

List of Figures

- Figure 1: Helicopter airborne time domain EM survey, transmitter loop emitting primary magnetic field, inducing secondary currents in target body (transmitter on)..... 4
- Figure 2: Figure 2 Helicopter airborne time domain EM survey, secondary magnetic field generated by the induced currents in target body, measured at receiver (transmitter off). The vector n is normal to the plane of the current flow4
- Figure 3: Simplified synthetic model of a sphere underlying conductive overburden showing electromagnetic parameters and body geometry (after Desmarais and Smith, 2016). 7
- Figure 4: A 3D representation of the dipping sphere model derived in Desmarais and Smith, (2016) where current flow is restricted to parallel planes within an anisotropic sphere..... 8
- Figure 5: Simplified flowchart of the semi-analytic sphere overburden solution as it is implemented in the program. 10
- Figure 6: Screenshot of the sphere-overburden program developed in C++ and python, GUI made using the PyQt5 framework..... 11
- Figure 7: GUI for the sphere-overburden modelling program, variables include, first or second order response, conductivity of sphere and overburden, overburden thickness and more..... 12
- Figure 8: The z-component of the electromagnetic response for a sphere, 100 m below surface with a conductivity of 1 S/m and overburden thickness of approximately 0m 16
- Figure 9: The z-component of the electromagnetic response for a sphere, 300 m below surface with a conductivity of 1 S/m and overburden thickness of approximately 0m 17

List of Figures

- Figure 10: The z-component of the electromagnetic response for a sphere, 100 m below surface with a conductivity of 1 S/m and overburden thickness of 20m 17
- Figure 11: The x- component of the electromagnetic response for a sphere at depth 300 m below surface with conductivity of 1 S/m. (a) Fugro result, the spacing between the major ticks is 200 m (x-axis) (b) sphere-overburden implementation. 19
- Figure 12: The x-component of the electromagnetic response for a sphere dipping at 135 degrees, 300 m below surface with a sphere conductivity of 1 S/m. (a) Fugro result, the spacing between the major ticks is 200 m (x-axis) (b) sphere-overburden implementation. 19
- Figure 13: The z-component of the electromagnetic response for a sphere at depth 300 m below surface with a conductivity of 1 S/m. (a) Fugro result, the spacing between the major ticks is 200 m (x-axis) (b) sphere-overburden implementation. 19
- Figure 14: The z-component of the electromagnetic response for a plate dipping at 135 degrees, 300 m below surface with a conductivity of 1 S/m. (a) Fugro result, the spacing between the major ticks is 200 m (x-axis) (b) sphere-overburden implementation..... 19
- Figure 15: HELITEM® B field z-component response (channel 28). Line 1075 indicated by the red line passes over the IR2 conductor..... 20
- Figure 16: HELITEM® transmitter reference waveform. 22
- Figure 17: Line 1075 of the HELITEM® data for time windows (1-30) on a logarithmic scale. The flight line passes over the IR2 conductor near 6416700N. Each profile corresponds to a delay time from 1.65 to 14.26 ms after shut off. Not all time windows at all locations. 23

List of Figures

Figure 18: Line 1075 of the HELITEM® data for time windows (21-29) on a linear scale. The flight line passes over the IR2 conductor near 6416700N. Each profile corresponds to a delay time from 2.58 to 11.46 ms after shut off..... 23

Figure 19: Results of the sphere-overburden modelling (dashed line) over lying the HELITEM® data (solid line) for Line 1075 showing the late time windows (22-29). The flight line passes over the IR2 conductor near 6416700N. 26

Figure 20: Maxwell model data (red) overlying VTEM Max data (black) from Macnae and Hennessy (2019) from flight line 1075 showing the response of the IR2 conductor at the Forrestania test site..... 28

Chapter 1

1 Electromagnetic geophysics methods

Electromagnetic (EM) prospecting is one of the most widely used methods in mineral exploration. The method was originally developed in the early 1900's in the United States, Canada and Scandinavia where it is common to find a large resistivity contrast between conductive bodies at depth and resistive background material, an ideal geologic setting for the detection of conductive bodies with EM methods (Telford et al, 1990). Airborne methods were later developed in the mid 1950's and were widely used to detect conductors over large areas in a more cost and time efficient manner than ground-based EM surveys (Telford et al, 1990). Both ground and airborne EM systems have configurations that differ in terms of system geometry, operating frequency, transmitter waveform and more. The variety of system configurations make different airborne systems uniquely suited for use in different settings, some of the most commonly used airborne systems include HELITEM®, VTEM, MEGATEM, HELISAM and others. Airborne EM systems are also developed for specific applications outside of mineral exploration, an example of this is the airborne EM system SKYTEM, which is widely used in hydrogeological applications for salinity mapping as the high signal-to-noise ratio and fast transmitter shut off allow for collection of high-resolution data in the near surface and an estimate of depth to the target body (Sørensen and Auken, 2004). Active source EM systems consists of a transmitter and receiver coil at or above surface, typically at a constant spacing. In the case of airborne EM the transmitter and receiver coils can be towed behind the aircraft or attached to the extremities of the aircraft for a fixed wing system. The variety of airborne EM systems further adds to the method's versatility and effectiveness as a tool for detecting conductive bodies at depth.

1.1 EM geophysics theory

The practice of EM surveying begins with generation of a primary field that penetrates into the subsurface. For the case of time domain EM methods, the primary field is associated with a bipolar current pulse flowing in a transmitter loop that repeats at a specific base frequency. The current waveforms can have the shape of a half sine-wave, step or ramp (Telford et al, 1990). The changing primary field generates electrical currents termed secondary currents in conductive material in the ground. These currents in turn, have an associated secondary magnetic field that propagates out from the conductive body and is measured at or above surface at the receiver producing a secondary field that generally decays with time (Telford et al, 1990). The secondary field is measured as a function of the delay time (after the transmitter shut off) in measurement intervals termed time windows and are traditionally numbered from early to late time. The amplitude and decay rate of the secondary field measured at the receiver provides information about contrasting physical properties of the subsurface, this contrast in physical properties allows us to detect conductive bodies at depth and make geological interpretations of the subsurface. Figures 1 & 2 depict the processes of EM induction that occurs in the subsurface during an airborne time-domain survey over a conductive body. Electromagnetic induction processes are governed by the Maxwell equations (Grant and West, 1965). A current driven through a transmitter (figure 1) has an associated primary magnetic field (Ampere's law). The current switches off after the transmitter pulse, this results in a time-varying magnetic field in the subsurface, which according to Faraday's law results in an electric field circulating around the primary magnetic field. If there is conductive material in the subsurface, then Ohm's law tells us that this electric field is proportional to an induced current flow within the conductive body. Ampere's law applied to the induced (secondary) current gives a secondary magnetic field (figure 2) that can be sensed at the receiver, typically during the transmitter off-time. The resolving power and overall success of any given EM geophysics survey is dependent upon how

the physical properties of the target vary from that of the background material. The physical properties of greatest relevance to EM methods are as follows (in order of importance): 1) electrical conductivity 2) magnetic permeability 3) dielectric permittivity (Telford et al, 1990). These physical properties will determine the time-decay curve of the secondary field measured at the receiver where, conductive bodies will have a slower secondary field decay rate. It is important to consider factors that impact conductivity and resistivity in the subsurface. The main factors that control electrical conductivity of the subsurface are; mineralogy, porosity and pore saturation. The electrical current within a rock will travel along the path of least resistance: in ore-bearing rocks the current will travel through any of the metal-oxides, metal-sulfides, native metals or any graphite present in the rock, avoiding the relatively resistive silicate minerals. Current can flow through these substances with little resistance as the outer electrons of the atoms that make up the materials are loosely bound and can move freely (Huebener, R., 2014). The magnetic permeability of geological environments has been shown to impact the response of EM surveys and must be accounted for when the target body has a high concentration of magnetite and pyrrhotite, which have very high magnetic permeabilities. The dielectric permittivity of a material is the ability of a given substance to hold an electric charge. In electromagnetic prospecting methods, the dielectric permittivity is assumed to be negligible, which is called the *quasi-static* assumption (Grant and West, 1965) These physical contrasts along with other properties such as depth to body, shape and orientation will determine if the EM survey is able to detect the target conductor. The results of an EM survey are interpreted by comparing the measured response over a profile to the calculated response of forward models consisting of various simple shapes with specific properties. Common configurations include a conductive sphere in a uniform or dipole field (Grant and West, 1965), or a plate (Dyck et al., 1980). Simple forward models are not always appropriate for responses measured in field surveying, it is therefore desirable to generate forward models that are representative of field

data settings, in terms of the stratigraphy and orientation of the underlying geology and its associated physical properties.

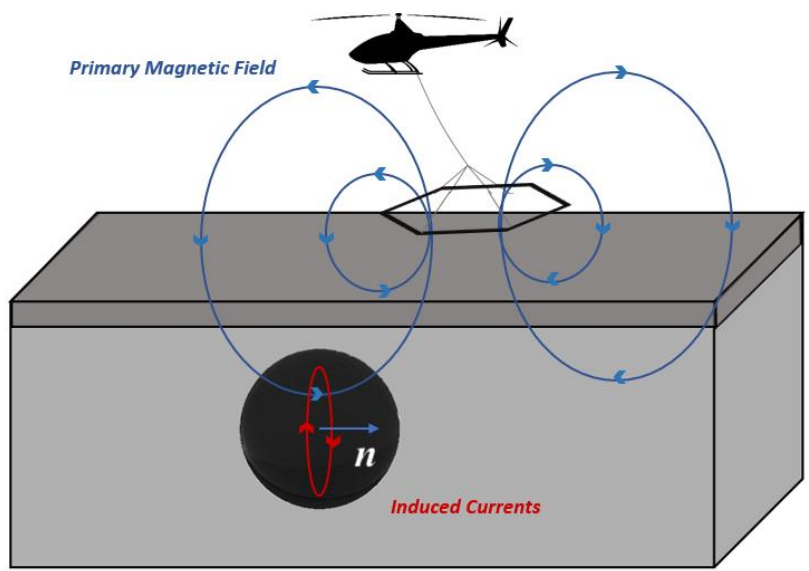


Figure 1: Helicopter airborne time domain EM survey, transmitter loop emitting primary magnetic field, inducing secondary currents in target body (transmitter on). The vector n is normal to the plane of the current flow

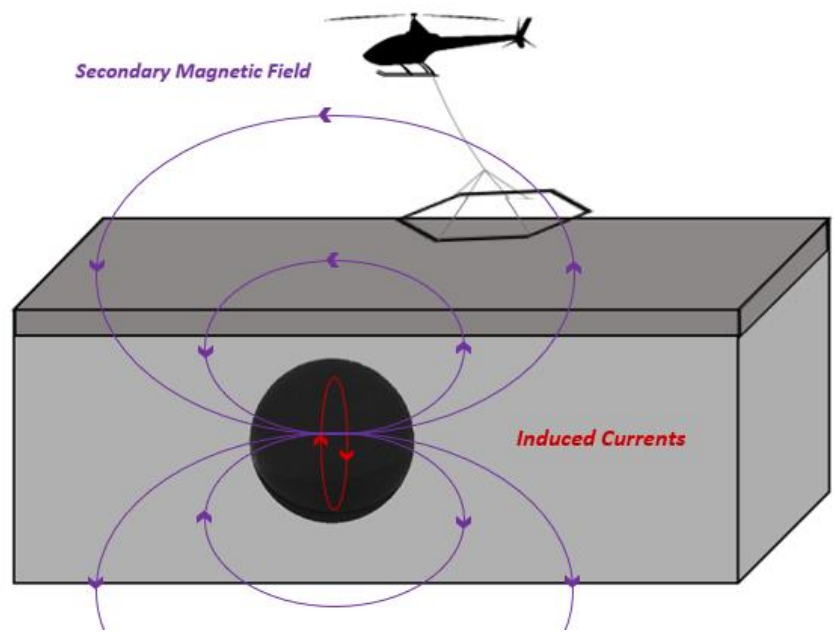


Figure 2: Helicopter airborne time domain EM survey, secondary magnetic field generated by the induced currents in target body, measured at receiver (transmitter off).

1.2 Discrete conductor models

Discrete conductor models in mineral exploration geophysics are useful for gaining an understanding of the response of highly conductive target bodies and can be used for the interpretation of airborne, ground or borehole EM data. For EM methods, the discrete target bodies in these forward models are most commonly represented as plate-like or spherical conductors (Lamontagne et al., 1988). It is possible to infer information about the parameters of the target body by fitting a discrete conductor model to acquired data or by directly analyzing the shape and decay of the EM response (Valleé, 2015), which is commonly used in the processing of airborne EM data. Plate models are most commonly used, as they are useful for representing thin and dipping conductors; however, for thicker, discrete conductors, sphere models are more appropriate, as the current can flow in multiple orientations perpendicular to the primary field (Dentith and Mudge, 2014). The mathematical formulations for discrete models in half-spaces and below overburdens (Raiche et al., 2007) can be complex and relatively computationally expensive. Hence, they have not been implemented into programs that can be used for interactively modelling EM responses.

The EM response of a small sphere in a uniform field (Grant and West, 1965) was adapted by Smith and Lee (2001) to model both sphere like bodies and spheres where the currents are constrained to flow in a plane with a specified strike and dip. The latter variant is able to mimic the response of dipping plates. This versatile model has been used for interpreting airborne EM data (Smith and Salem, 2007; Desmarais and Smith, 2015a) and determining the cross-sections of investigation associated with specific EM systems (Smith and Wasylechko, 2012; Desmarais and Smith, 2015b).

1.3 Research goals

In mining geophysics, we are often interested in the case of a discrete conductor embedded in a resistive environment or half-space. This situation is common in the Canadian shield, where conductive massive sulfide orebodies are embedded in resistive metamorphic or igneous rocks. If there is a conductive overburden above this resistive half-space, then it is important to account for the interaction between the discrete conductor and the upper layer of conductive overburden (Desmarais and Smith, 2016). A simplified model for the case of a sphere underlying conductive overburden is shown in figure 3. A semi-analytical solution for this model was derived in Desmarais and Smith (2016) and is implemented in our modelling software. The program can quickly generate the airborne EM response for synthetic models such as the model presented in figure 1. In normal sphere solutions, the EM current flow is perpendicular to the vector \mathbf{n} , which is parallel to the time-varying magnetic field exciting the sphere. However, the response of plate-like bodies can also be approximated by specifying that the induced current can only flow at a specific orientation. This is what would occur if the sphere was comprised of multiple thin layers with alternating conductive and resistive material. Such a sphere is essentially anisotropic, with current only being able to flow in the plane of the conductive layers and not in the perpendicular direction. For brevity, we call this model a “dipping sphere”. A 3D representation of this model is presented in figure 4 where the induced currents flow within parallel planes, in this case slightly off vertical. The ability of this model to be representative of a plate-like or spherical body interacting with conductive overburden makes it a uniquely versatile model (Smith and Lee, 2001).

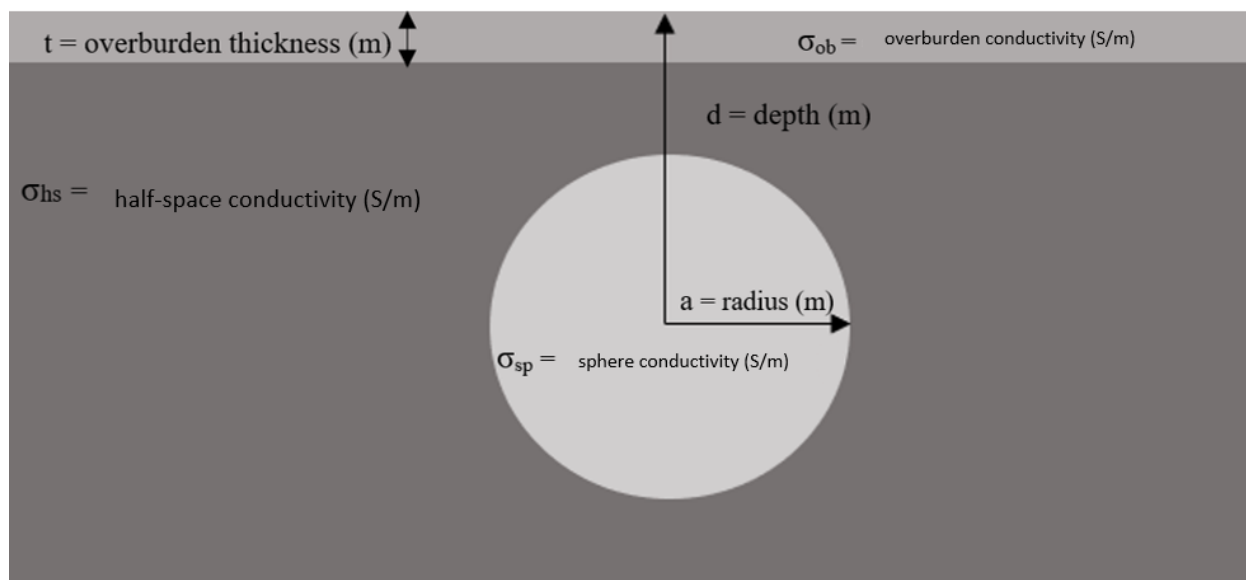


Figure 3: Simplified synthetic model of a sphere underlying conductive overburden showing electromagnetic parameters and body geometry (after Desmarais and Smith, 2016).

The response of the dipping sphere buried below overburden can be calculated in a few seconds on a laptop computer. This provided us with an opportunity to create an interactive computer program that could be used for multiple purposes:

- 1) for students to learn how the EM response varies when various parameters of the model, e.g. dip, depth, overburden conductivity;
- 2) for geophysicists to test whether the response of an expected target would be evident above the response of the overburden or the noise levels; and
- 3) for geophysicists to adjust the acquisition parameters, such as the base frequency to a system so that their target could be identified on an EM survey.
- 4) For geophysicist to explain a measured response by adjusting the parameters of the model until the model response is similar to the measured response.

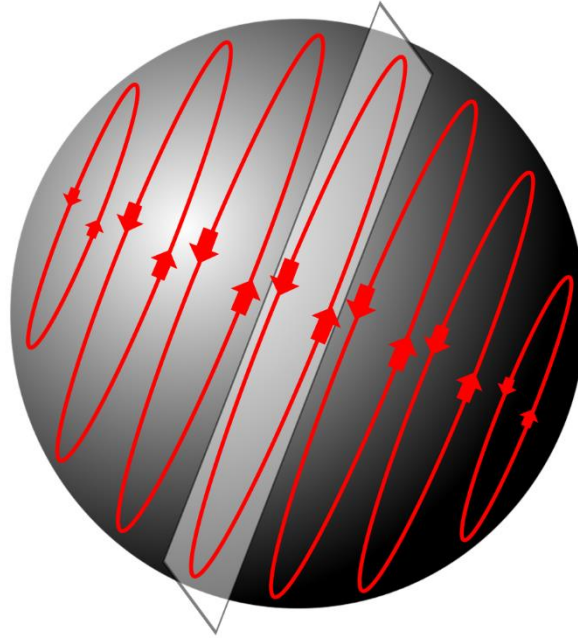


Figure 4: A 3D representation of the dipping sphere model derived in Desmarais and Smith, (2016) where current flow is restricted to parallel planes within an anisotropic sphere.

Chapter 2

2 Sphere-Overburden algorithm

The semi-analytic solution of Desmarais and Smith (2016) assumes that the combined response of the sphere and overburden is reasonably approximated by a sphere excited by the currents induced in the overburden. This approximation was proposed in Liu and Asten (1993) using the estimated response of a wire loop interacting with conductive overburden. They argued that the response may be written as the overburden field H_{ob} plus a sum of terms H_n accounting for the inductive interaction between the sphere and overburden.

$$H = H_{ob} + \sum_{n=1}^{\infty} (H_n)$$

Liu and Asten (1993) demonstrated that using only the first-order term

$$H \approx H_{ob} + H_1$$

gave a reasonable approximation as the magnitude of the higher-order terms (H_2 , H_3 , etc) are progressively weaker. The first-order term assumes that the sphere response is excited by the secondary field of the currents induced in the overburden. The sphere-overburden algorithm also assumes that the sphere is not in contact with the overburden, so there is no channeling of overburden currents into the sphere. The formulation also assumes that the sphere is a dipole in a uniform field, which Smith and Lee (2001) argued was reasonable for the airborne EM configuration, where the transmitter and receiver are normally a large distance from the target. These approximations greatly reduce computation time as the response at each location may be calculated by convolving the overburden response with that of the target, which is a sum of decaying exponentials (Desmarais and Smith, 2016). The short computation time will allow many electromagnetic responses to be generated along a profile quickly. Our initial efforts have been to model the response of airborne EM systems with arbitrary waveforms and geometries. The arbitrary waveform is accounted for by a second convolution integral, where the impulse response of the sphere-overburden is convolved with the EM system current waveform. Airborne EM systems generally only have one or two receiver positions for each transmitter dipole location on the profile. However, the program could be adapted for ground EM systems, which generally have one large loop transmitter position and multiple receiver positions (e.g. Desmarais and Smith, 2015b). A simplified flowchart of the response calculations made by the sphere-overburden program is presented below in figure 5.

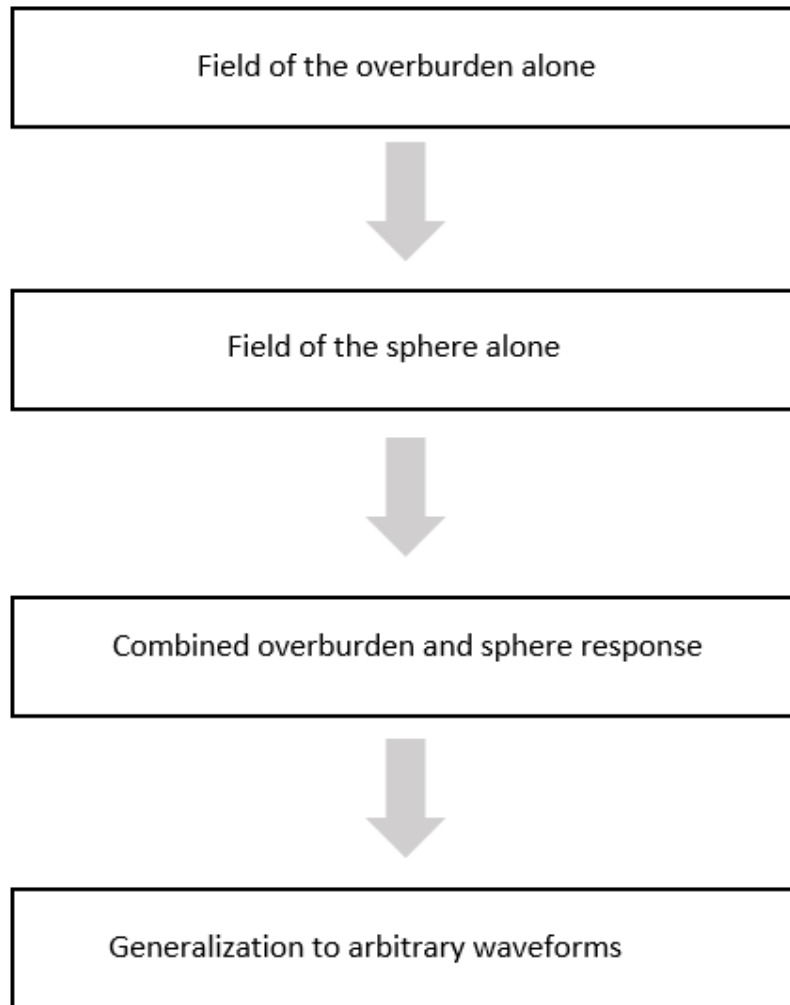


Figure 5: simplified flowchart of the semi-analytic sphere overburden solution as it is implemented in the program.

Chapter 3

3 Program Design

The sphere-overburden program was written in C++ and python, the program was designed to provide a user friendly and fast method of modeling airborne EM responses. A screen capture of the programs graphical user interface (GUI) is presented in figure 6. The screen shot presents the z-component response calculated and plotted on the right-hand side of the image, given the user defined parameters on the options widget on the left-hand side of the screen.

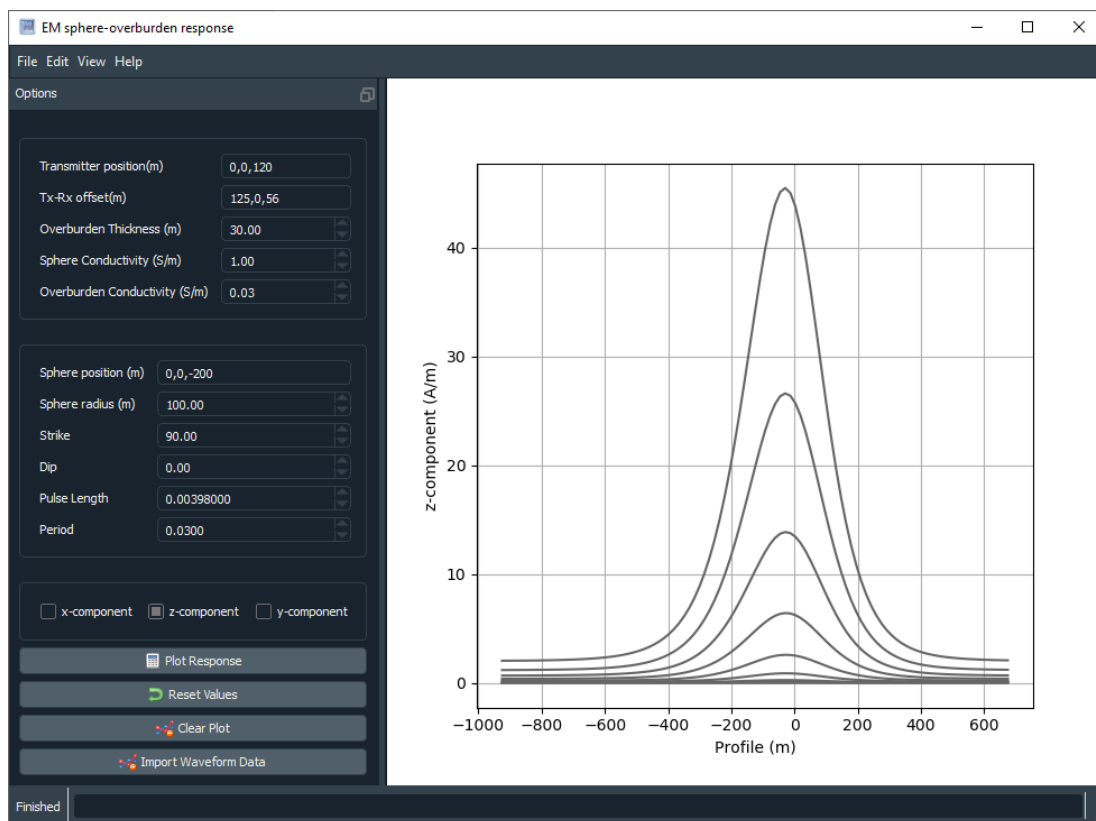


Figure 6: Screenshot of the sphere-overburden program developed in C++ and python, GUI made using the PyQt5 framework

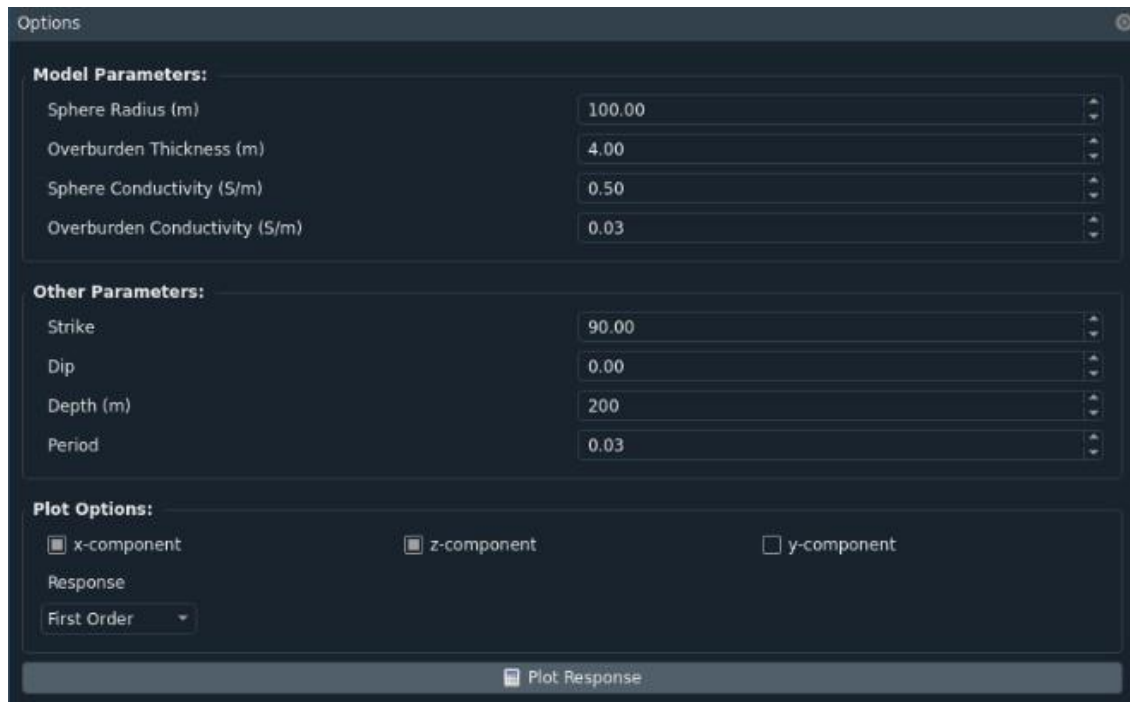


Figure 7: GUI for the sphere-overburden modelling program, variables include, first or second order response, conductivity of sphere and overburden, overburden thickness and more

Figure 7 removes the plotting area from figure 6 to highlight some of the system parameters that can be manually changed by the user using the GUI, including the transmitter position relative to the plotting point, the receiver position, relative to the transmitter. Note that the offsets are assumed to be positive when the receiver is to the left of the transmitter for the x offset, into the page for the y offset and up for the z offset. If negative offsets are used, then the sign of the response may be different from expected as the x component is defined as having a positive response in the direction to the right, but some airborne EM systems define a positive x response as being in the direction from the transmitter to the receiver.

Other variables the user is able to change via the GUI include the sphere radius, conductivity, depth and overburden thickness and conductivity. Note however, that the algorithm assumes a thin-sheet approximation for the overburden (Grand and West, 1965), so entering a greater thickness and correspondingly smaller conductance will give identical results.

The GUI can also be used to specify the survey parameters such as the dip, strike, transmitter dipole moment, transmitter base frequency and profile length. When the dip is specified to be zero then the “dipping sphere” model is not used and the normal sphere models is used, where the currents flow perpendicular to the direction of the excitation field from the currents induced in the overburden. The components of the response to be plotted are selected using the corresponding x, y, z component buttons located underneath the system variables widget, the program allows for multiple components to be plotted at the same time to allow the user to quickly and easily compare between the x,y and z component of the airborne EM response. The function buttons at the bottom left of the GUI presented in figure 7 allow the user to control the functionality of the program including generating the responses, clearing the plots and resetting the parameter values to default. The import waveform button allows to user to import time window data and transmitter current pulse data in the form of a csv file. The corresponding data sets are read into the program and used in the sphere-overburden routine to generate a response for a specific EM system.

3.1 Program development

This user interface was written in python using the PyQt5 framework, parts of the response computation functions were written in C++ to take advantage of the computational efficiency that can be achieved using a programming language that uses a compiler to generate object code. Multiple code libraries and frameworks were used in the development of the sphere-overburden program, the open source C++ library Eigen was used for its linear algebra functionality and Pybind11 was used to wrap the C code in python. The python library Quadpy was used for its implementation of the Gauss-Kronrod numeric integration routine (used for convolution), which offers a large improvement in runtime over standard integration methods. Implementing performance-based libraries and frameworks in the software provides significant performance increases over interpreted languages for scientific or numerical programming. The sphere-overburden code was profiled and compared to an earlier implementation of the sphere-overburden calculations programmed in Matlab, a widely used interpreted language in the science and engineering community. Two EM responses were generated, one response is the impulse response and the second involved convolving the impulse response with a transmitter current pulse defined using a 400-point time series. The C++/python implementation calculated the impulse response in 4 seconds compared to 20 seconds for the Matlab implementation. When convolving with the transmitter waveform data, the C++/python implementation generated a response in 3 minutes while the Matlab implementation completed in 12 minutes. These times are of course machine dependent. The use of optimized open-source libraries and compiled code provides a sphere-overburden solution that is fast and convenient for the end user. All libraries and frameworks used are open source and covered under the MIT license. The program is compiled to a windows executable using the pyinstaller library, this allows for easy distribution of the software.

Chapter 4

4 Methods

Airborne EM data in its raw form can be problematic for inexperienced people to interpret, particularly if they do not have access to geophysics modelling software. Hence, the data will often be processed and converted to data formats that are more readily interpretable such as conductivity depth images (CDI) or perhaps even 2D or 3D inversions. These images and inversions require a starting forward model to produce good results. Simple starting models such as half spaces are sometimes used, but for discrete conductive bodies, the most geologically reasonable results are obtained if the starting model is also a discrete conductor and has a reasonable fit to the data. Hence a simple sphere-overburden model might be a good starting model, even when the actual situation is more complex (not a sphere or not in a resistive host). One way to generate such appropriate models for airborne EM profiles is by fitting the anomalies observed along a flight line using modelling software such as the Maxwell plate modelling software (<http://www.electromag.com.au/maxwell.php>) or the Multiloop modelling package (<https://www.lamontagnegeophysics.com/products-multiloop-home.html>). The sphere-overburden program provides another modelling software package that can easily include conductive overburden and allows the flexibility of spheres and dipping spheres. It is an accessible tool that can be used for fast modelling prior to using more sophisticated tools such as Maxwell or Multiloop, that allow modelling using multiple lines, multiple bodies, etc.

4.1 Synthetic models

The sphere-overburden program is able to generate EM responses over a sphere or dipping plate with user-defined model parameters, these synthetic models allow users to see the resulting changes in the shape and amplitude of the EM response. Figures 8-10 are synthetic sphere models that show the z-component of the EM response for varying sphere depths and overburden thicknesses. Comparing figure 8 and figure 9 it is seen that as the sphere depth is increased from 100 m to 300 m the amplitude of the response decreases and the peak of the anomaly becomes more broad, there is no overburden response as the thickness of the overburden in these models is set to be a negligible thickness. Comparing figure 8 to figure 10 it is observed that when an overburden is introduced to the model the early-time channels increase in amplitude; this is most evident on either side of the sphere.

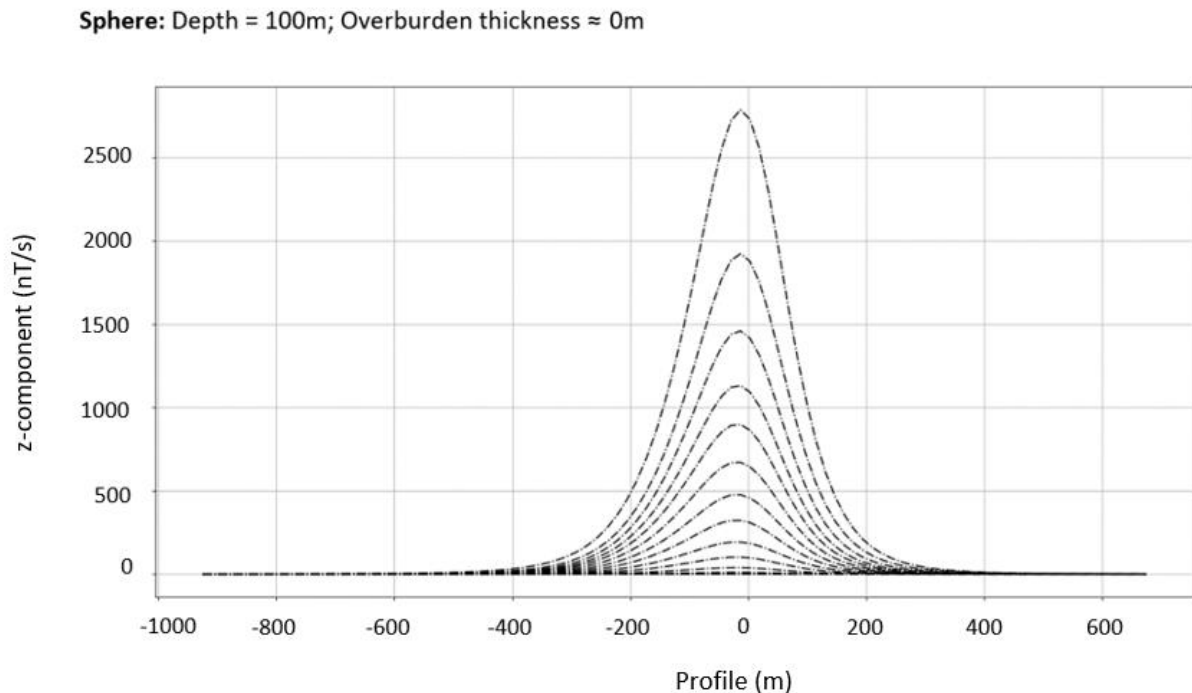


Figure 8: The z-component of the electromagnetic response for a sphere, 100 m below surface with a conductivity of 1 S/m and overburden thickness of essentially 0 m

Sphere: Depth = 300m; Overburden thickness \approx 0m

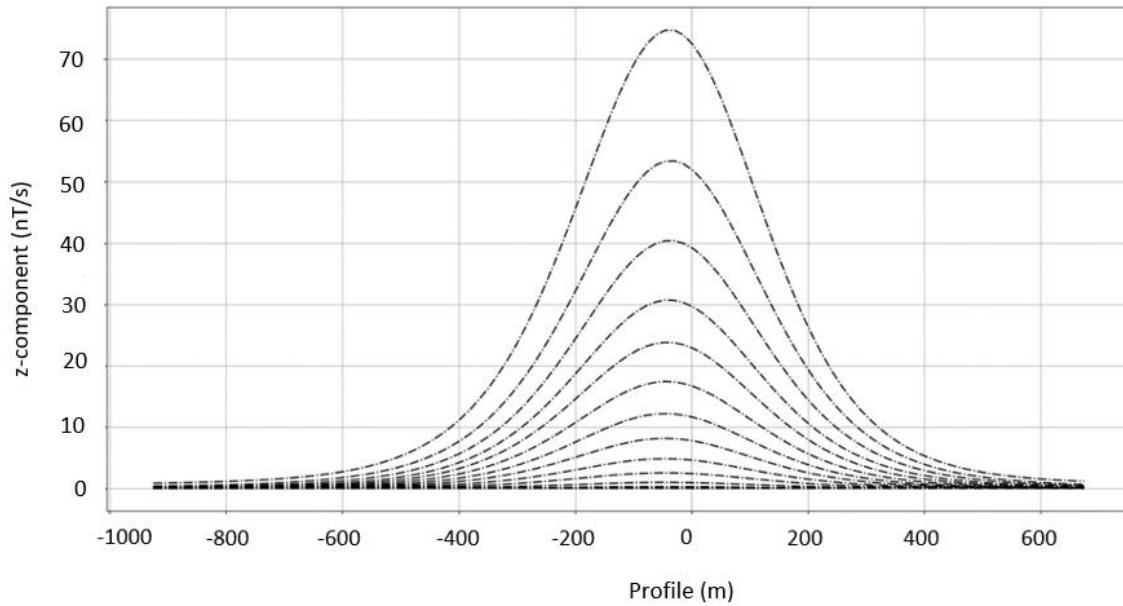


Figure 9: The z-component of the electromagnetic response for a sphere, 300 m below surface with a conductivity of 1 S/m and overburden thickness of essentially 0 m

Sphere: Depth = 100m; Overburden thickness = 20m

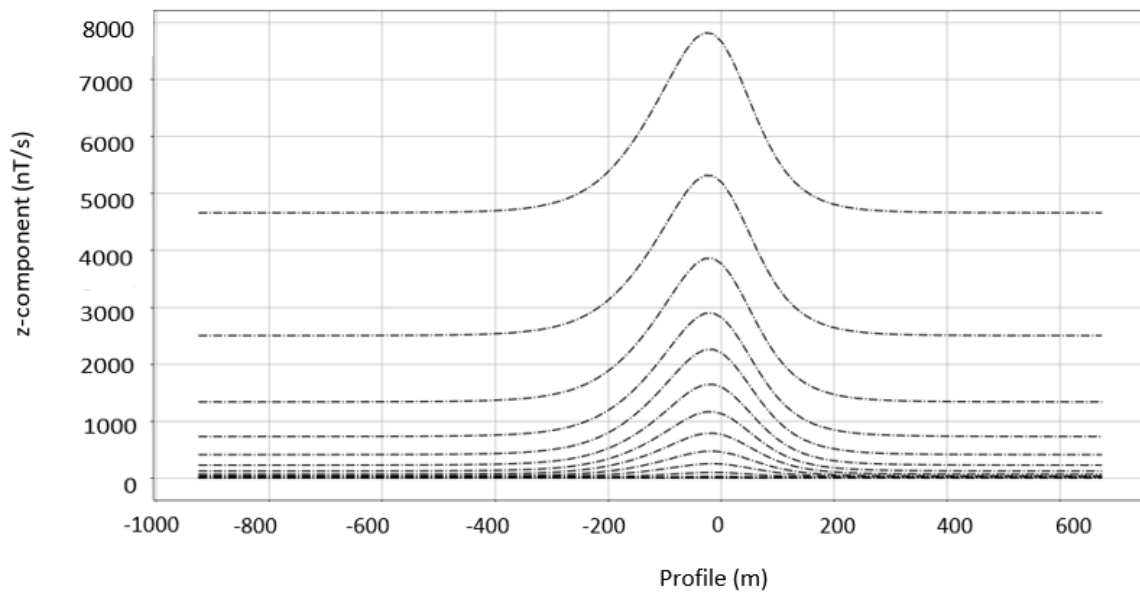


Figure 10: The z-component of the electromagnetic response for a sphere, 100 m below surface with a conductivity of 1 S/m and overburden thickness of 20 m

To validate the EM responses generated by our program, we compare the results of the program with synthetic models generated by Fugro and presented in Slattery and Andriashek (2012), for both a sphere model and a dipping-sphere model. The synthetic models were presented as part of a 2012 open file report describing airborne EM and magnetic data collection using the GEOTEM system in Alberta. The synthetic models presented in the report were generated using the sphere in a uniform field algorithm derived in Smith and Lee, (2001), but adapted to the time domain, using the formulation of Smith and Neil (2013). The x- and z-components of the response for a sphere and dipping-sphere in free space with no conductive overburden as presented in Slattery and Andriashek (2012) are shown in figures 11-14 (a). The response generated by our implementation are shown in figures 11-14 (b). Figures 11 and 12 are for the x-component, figures 13 and 14 are for the z-component. It is seen that for both, the case of the dipping-sphere and sphere model, the shape of the response in the x- and z-components produced by our program is in agreement with those of Slattery and Andriashek (2012). The amplitude of the plots is not expected to be in agreement due to uncertainty in system parameters, the dipole moment and sphere radius used to generate the Fugro responses were not specified in Slattery and Andriashek (2012). Additionally, the EM responses generated by Fugro used a sphere model which has no conductive cover, to compensate for this the overburden thickness parameter of the sphere-overburden algorithm is set to be a negligible thickness. There is some discrepancy in the amplitude of the responses, overall, this comparison confirms that key aspect of the sphere-overburden program have been implemented correctly, further validation efforts using more representative models would be beneficial.

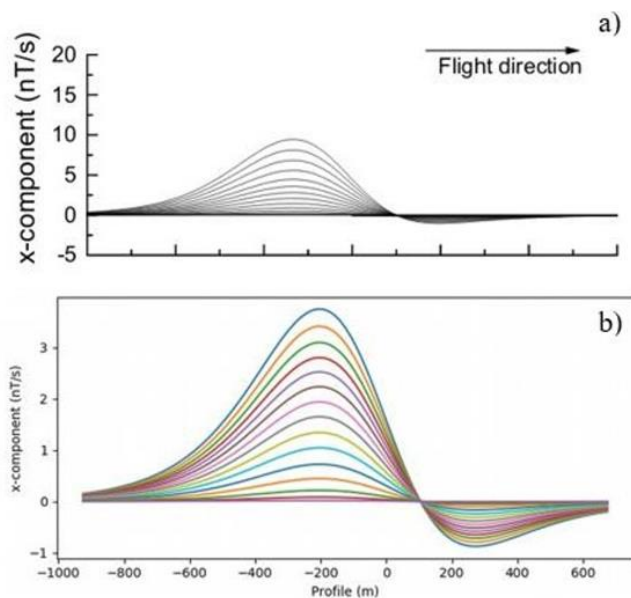


Figure 11: The x - component of the electromagnetic response for a sphere at depth 300 m below surface with conductivity of 1 S/m. (a) Fugro result, the spacing between the major ticks (x -axis) is 200 m (b) This implementation.

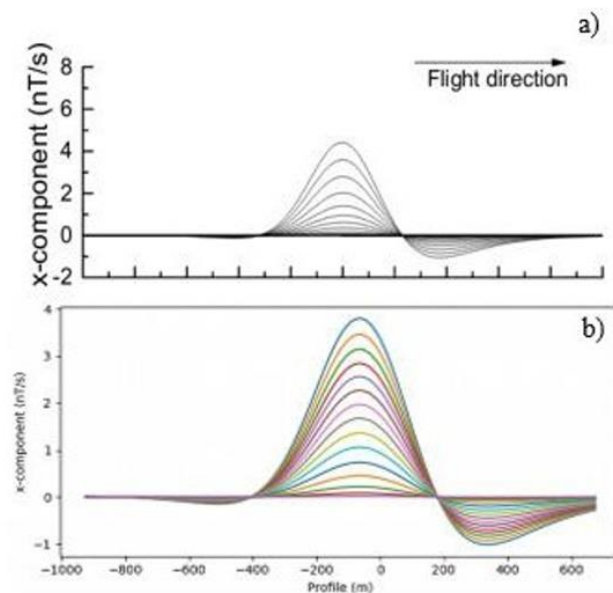


Figure 12: The x -component of the electromagnetic response for a sphere dipping at 135 degrees, 300 m below surface with a sphere conductivity of 1 S/m. (a) Fugro result, the spacing between the major ticks (x -axis) is 200 m (b) This implementation.

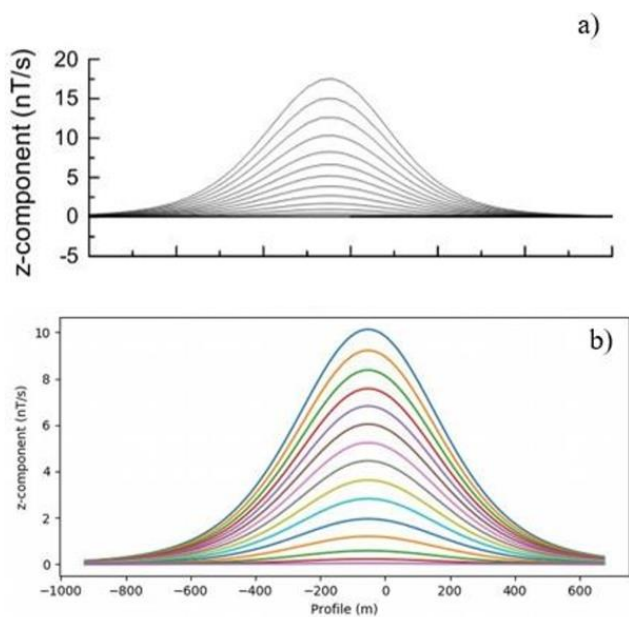


Figure 13: The z -component of the electromagnetic response for a sphere at depth 300 m below surface with a conductivity of 1 S/m. (a) Fugro result, the spacing between the major ticks (x -axis) is 200 m (b) This implementation.

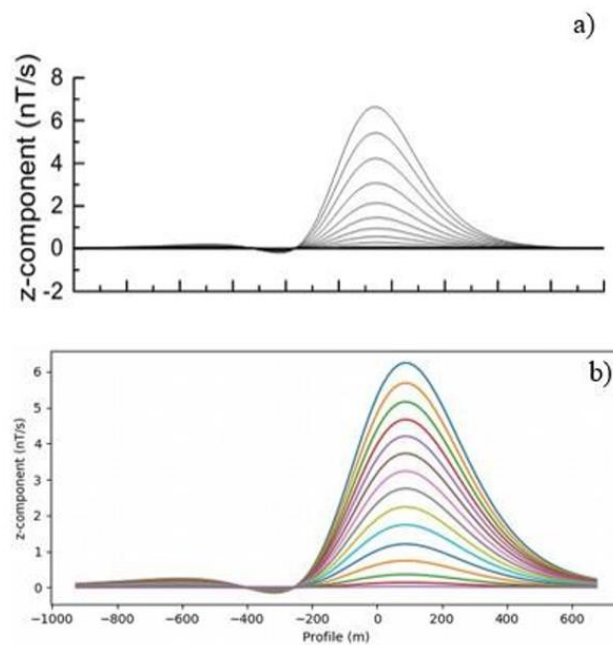


Figure 14: The z -component of the electromagnetic response for a plate dipping at 135 degrees, 300 m below surface with a conductivity of 1 S/m. (a) Fugro result, the spacing between the major ticks (x -axis) is 200 m (b) This implementation.

4.2 Modelling field data

In the *Research goals* section, four reasons were enumerated for developing the program. It is fairly straight forward to imagine how the program would be used to achieve the first three goals. Users can adjust the parameters of the bodies and the EM acquisition system in the GUI in order to observe the changes in the response profiles and how the calculated amplitudes compare with those of the overburden response and the noise levels. In this section we show how the newly developed sphere-overburden program, can be used to achieve the fourth goal, of modelling field data recorded over a known anomaly. The airborne data set was selected based on two main criteria. Firstly, the survey target should include a well constrained, well defined conductor that has been identified using multiple EM systems. Secondly, the survey area should have a regional geology that is representative of a discrete target with an underlying conductive overburden.

4.3 Forrestania test site

The Forrestania site includes a group of Ni-Cu deposits located approximately 400 km east of Perth in Western Australia (Prichard et al, 2013). Test ranges such as Forrestania present an opportunity for objective comparison and assessment of multiple types of airborne EM systems and their different specifications and system geometry (Gilgallon et al, 2019). The Forrestania test range is located on open, readily accessible land making it an ideal location for ground, airborne and borehole EM surveys, and hence, there has been numerous EM surveys and drilling carried out on the test site resulting in well-defined conductors and geology in the area with associated ground truth (Gilgallon et al, 2019). One of the surveys flown over the Forrestania EM test range was completed using the HELITEM® time domain airborne system.

Figure 15 presents HELITEM® B field z-component (dB/dt) data that has been collected over Forrestania and gridded. The red line shown in figure 15 depicts the flight line 1075 which passes over the IR2 conductor. The HELITEM® system is able to detect the response due to the shallow IR2 conductive body, the survey was also able to measure the response of more conductive material to the north of the IR2 conductor that is attributed to conductive overburden.

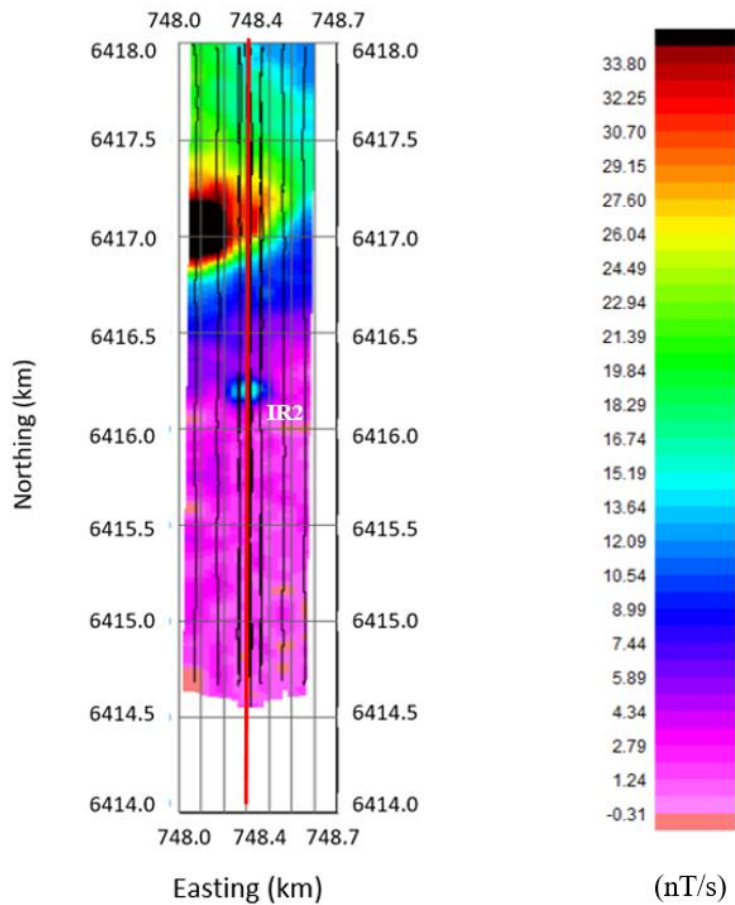


Figure 15: HELITEM® B field z-component response (channel 28). Line 1075 indicated by the red line passes over the IR2 conductor.

4.4 HELITEM® data

HELITEM® data collected over the Forrestania test site was provided by CCG for use in this modelling exercise. The HELITEM® system is an airborne time-domain EM system often used in environmental and mineral exploration applications (Hodges et al, 2016). The data set consist of 11 flight lines of 30 windows (listed in Table 1) measuring dB/dt. For this survey, the HELITEM® system was operating at a base frequency of 25 Hz with a sampling frequency of 102400 Hz, the transmitter current pulse is plotted in figure 16. Flight line 1075 of the HELITEM® data set was chosen for modelling the response over the IR2 conductor using the sphere-overburden program. Figure 17 shows the z-component profile on a log scale with the anomaly associated with the IR2 conductor evident at 6416700N. The data is first plotted on a log scale where all windows can be seen at once, so the conductor response can be seen in the context of the large overburden response at early time. The relative strength of the conductor anomaly relative to the overburden is greatest in the late time windows with increasing noise becoming evident in the very late windows. Hence, we model the late time windows (21 to 29) when trying to explain the response of the IR2 conductor with the sphere-overburden program. These windows can be seen on figure 18, where the response of the IR2 conductor is evident in the context of a rapid rise in amplitude to the north, attributed to conductive overburden. To generate a model to fit the HELITEM® data, we use the ‘read in waveform’ feature of the sphere-overburden program to import the reference HELITEM® waveform data, and the time windows in csv format. The transmitter reference waveform is convolved with the impulse response to generate the model response as described in Desmarais and Smith (2016).

HELITEM® window mid-times (ms)		
Ch 1-4 – on time data	Ch 13 – 0.605	Ch 22 – 3.10
Ch 5 – 0.165	Ch 14 – 0.725	Ch 23 – 3.73
Ch 6 – 0.195	Ch 15 – 0.865	Ch 24 – 4.50
Ch 7 – 0.225	Ch 16 – 1.035	Ch 25 – 5.42
Ch 8 – 0.260	Ch 17 – 1.235	Ch 26 – 6.53
Ch 9 – 0.305	Ch 18 – 1.480	Ch 27 – 7.88
Ch 10 – 0.360	Ch 19 – 1.785	Ch 28 – 9.50
Ch 11 – 0.425	Ch 20 – 2.145	Ch 29 – 11.46
Ch 12 – 0.505	Ch 21 – 2.580	Ch 30 – 14.26

Table 1: Time windows (in ms) used for the HELITEM® system when acquiring the Forrestania data

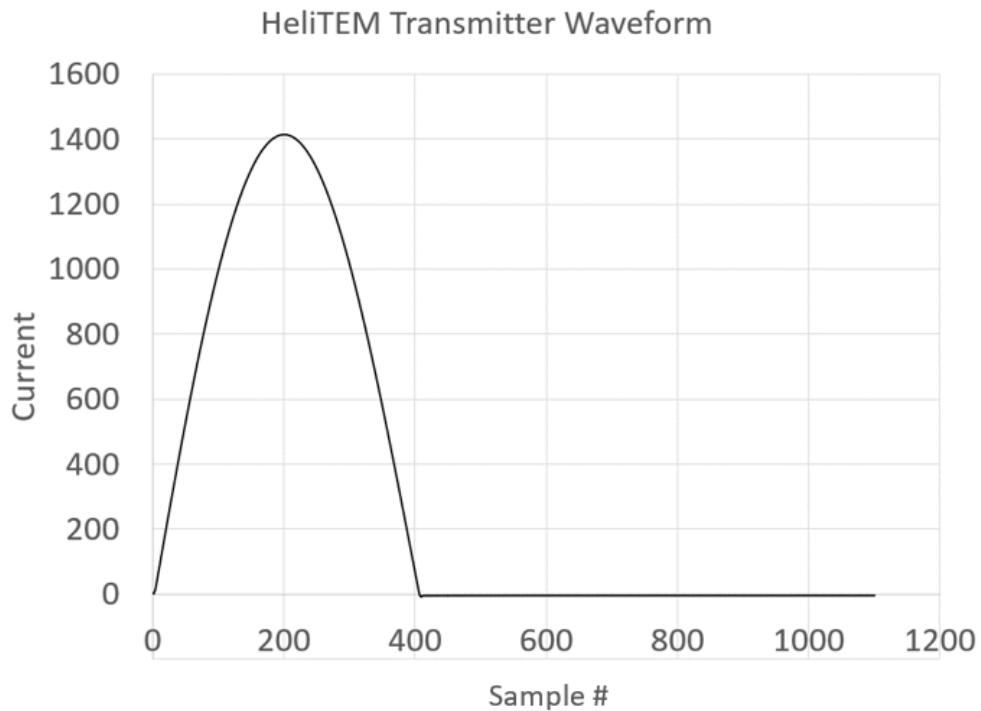


Figure 16: HELITEM® transmitter reference waveform.

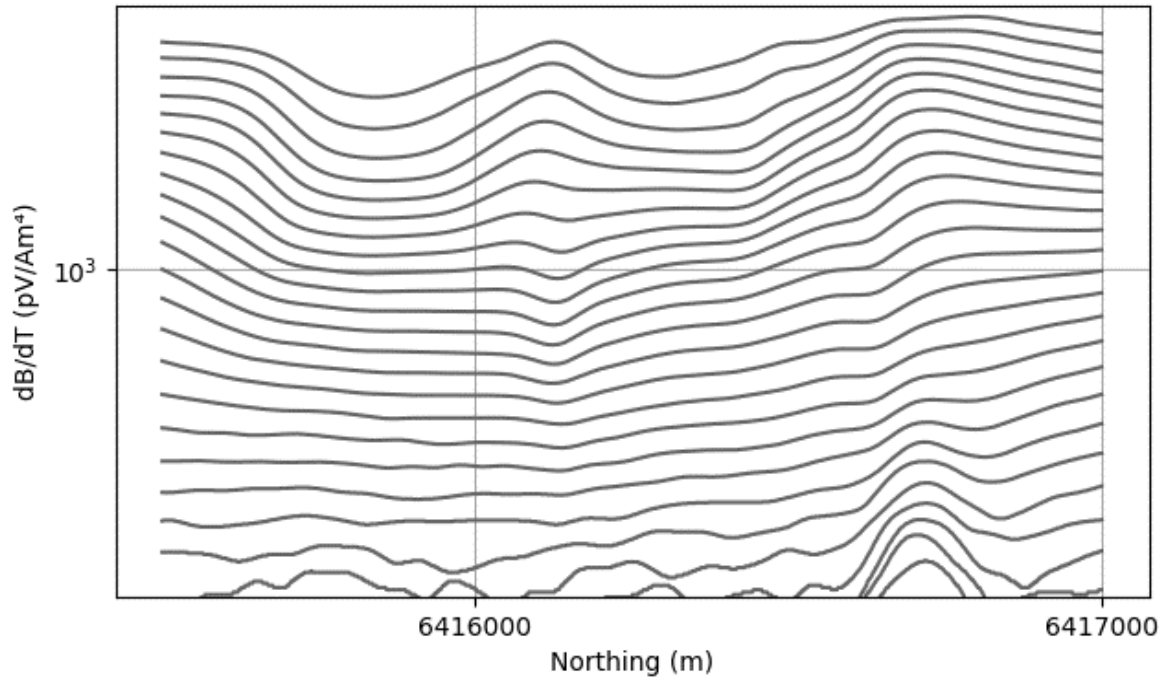


Figure 17: Line 1075 of the HELITEM® data for time windows (1-30) on a logarithmic scale. The flight line passes over the IR2 conductor near 6416700N. Each profile corresponds to a delay time from 0.165 to 14.26 ms after shut off. Not all time windows are evident at all locations.

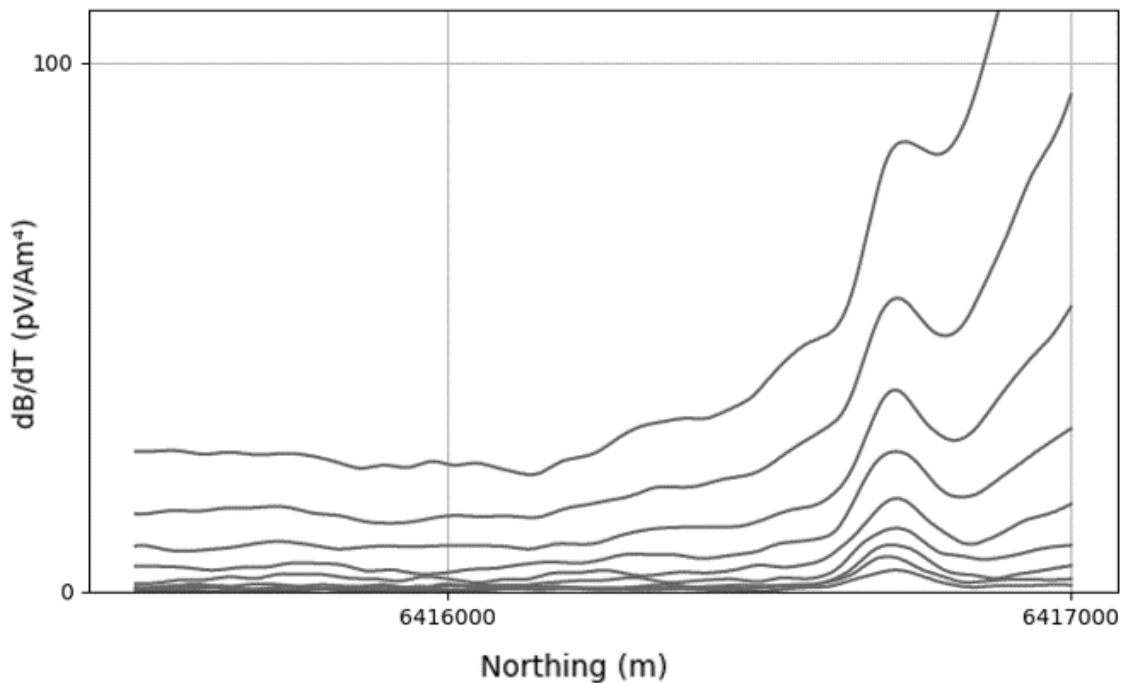


Figure 18: Line 1075 of the HELITEM® data for time windows (21-29) on a linear scale. The flight line passes over the IR2 conductor near 6416700N. Each profile corresponds to a delay time from 2.58 to 11.46 ms after shut off.

Chapter 5

5 Forrestania modelling results

The z-component of the data was chosen to be modelled as it shows the best coupling with the IR2 conductor resulting in the strongest signal-to-noise ratio at the latest time windows. The parameters of the model were manually adjusted in the sphere-overburden program to produce the best fit to the data. The results of the modelling are presented in figure 19, where, the response generated by the program is presented using dashed lines and is overlying the HELITEM® data which is presented using solid lines. In order to show a comparison of the model response with the overburden response on line 1075, the model data has been plotted 300 m on either side of the IR2 conductor. The model parameters for this model are listed in table 2. The body is given a dip of 35 degrees north and is located at a depth of 156 m to the center of the conductor body. The radius of the body was set to 46 m with a conductivity radius squared value (CRS) of 6624 Sm; the overburden is assigned a thickness of 57 m and conductivity of 0.05 S/m. Interpretation of independent EM surveys have estimated a model with a depth of less than 100 m, dipping at approximately 30 – 40 degrees north with a conductance greater than 7000 S (Gilgallon et al, 2019). The parameters of the response generated using the sphere-overburden program are mostly in agreement with the estimates given in Gilgallon et al, (2019), with the exception of a slightly larger depth to target of 156 m in our modelling results and the fact that for a sphere model we estimate a CRS rather than a conductance.

The values used to generate the response were manually tuned to achieve the most accurate fit of the response over the IR2 anomaly, the response generated by the sphere-overburden are non-unique, meaning that there are multiple combinations of model parameters (overburden thickness, overburden conductivity, sphere radius, sphere conductivity) that could produce the same response. The overburden response is larger than the model on the north hand side, but smaller on the south, so the overburden parameters represent a suitable compromise for both sides. Note that the width of the fitted data and measured data are comparable at all delay times.

Forrestania sphere-overburden model parameters	
Depth (m)	156
Strike (degrees)	90
Dip (degrees)	35
Radius (m)	46
Conductivity radius squared (Sm)	6624
Overburden thickness (m)	57
Overburden conductivity (S/m)	0.05

Table 2: Model parameters used in the modelling of the IR2 conductor response at the Forrestania EM test range using the sphere-overburden program.

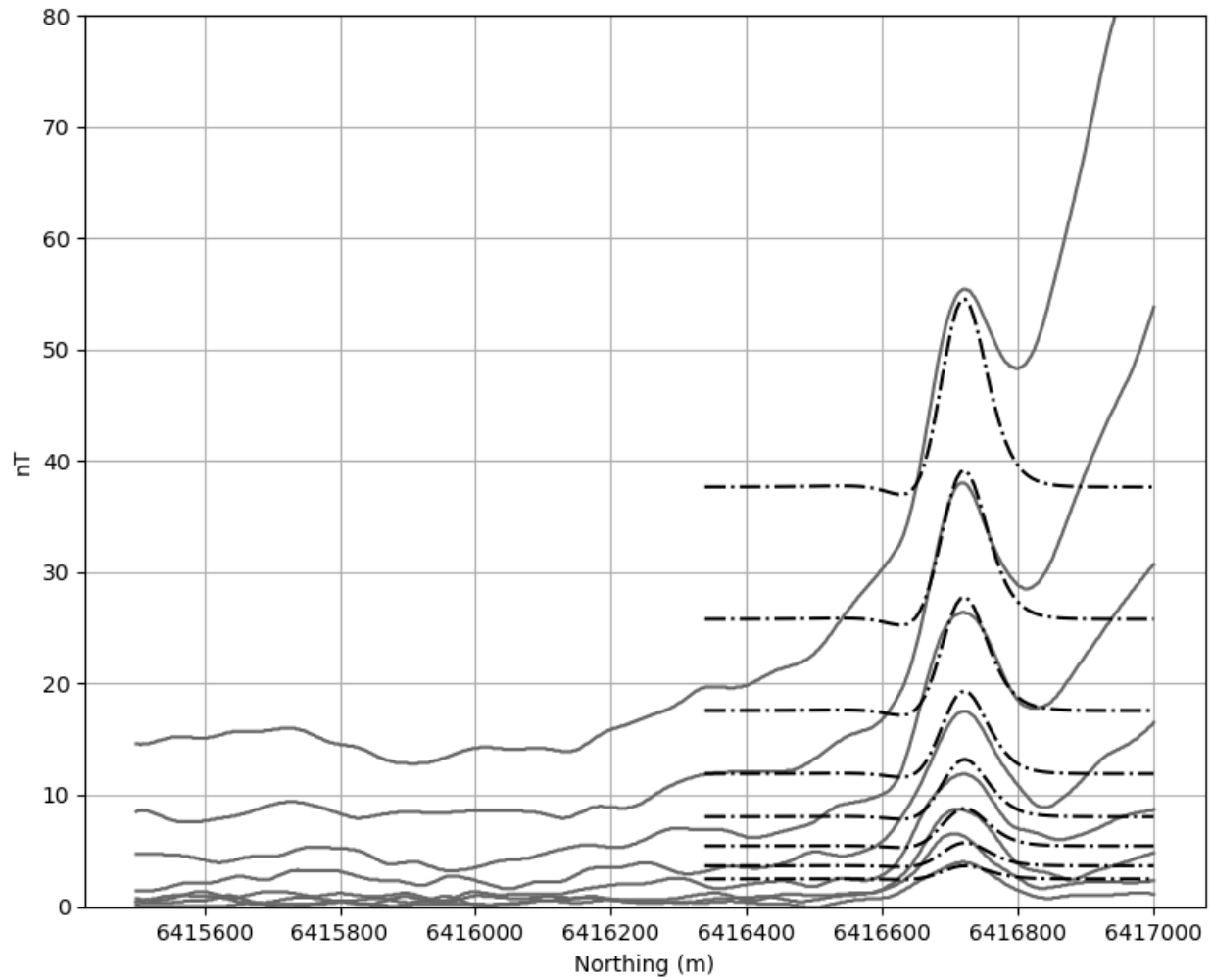


Figure 19: Results of the sphere-overburden modelling (dashed line) overlying the HELITEM® data (solid line) for Line 1075 of the for the late time windows (22-29). The flight line passes over the IR2 conductor at the Forrestania test site.

5.1 Comparison to Maxwell model

The results of the Forrestania models generated using the newly developed sphere-overburden program are compared to published modelling exercises completed on similar data. In Macnae and Hennessy (2019) modelled VTEM Max data over the IR2 conductor. The goal of the modelling in Macnae and Hennessy (2019) was to compare three different modelling algorithms. One of the algorithms used in Macnae and Hennessy (2019) was the Maxwell plate modelling software. The late delay-time windows of the VTEM Max data over a 2.5 km segment of the flight line (black lines) and the Maxwell model result (red lines) are presented in figure 20. Compared with the measured response, the Maxwell model appears too narrow, particularly at the earlier delay times, which is observed in the uppermost profile lines in figure 20 having an increasingly less accurate fit to the VTEM Max data.

The amplitudes are also slightly too large in the earlier windows shown in figure 20, so these aspects of the Maxwell model are not as good as the sphere-overburden model. Further, the Maxwell response on the immediate north and south is too small, whereas the sphere-overburden model was too large to the south and too small to the north. The Maxwell model shows an increase further to the north, perhaps because of a second conductor was placed to the north to try and model the overburden. With further effort it might have been possible to improve the fit to the overburden in the Maxwell model, but modelling multiple bodies can be difficult, particularly if there is inductive interaction. It was concluded by Macnae and Hennessy (2019) that the Maxwell model would be too unstable for use in an inversion algorithm.

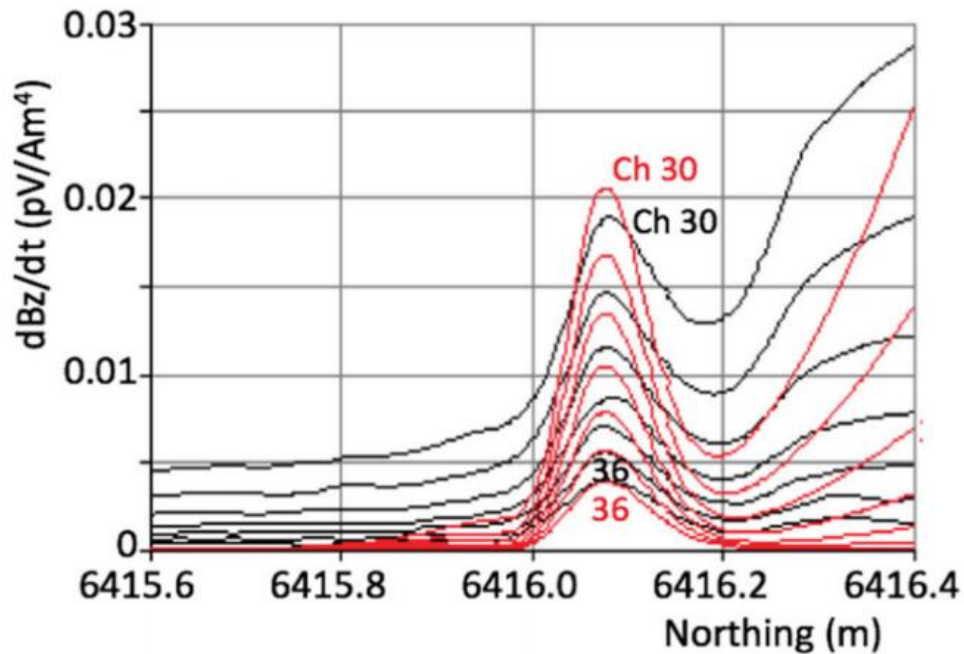


Figure 20: Maxwell model data (red) overlying VTEM Max data (black) from Macnae and Hennessy (2019) from flight line 1075 showing the response of the IR2 conductor at the Forrestania test site.

Both the Maxwell and sphere-overburden models fail to accurately model the response on either side of the IR2 anomaly. In this case, the large variance in overburden thickness and conductivity results in an unsuitable response using both programs. While we presume that the Maxwell model attempts to improve the fit with an extra body to the north, the sphere-overburden program is unable to account for rapid variations in thickness and conductivity of the overburden and is only able to model a constant response for the conductive cover. These results suggest that the sphere-overburden modelling software is capable of achieving a good fit to data in an environment with constant overburden conductance.

Chapter 6

6 Discussion and future work

The sphere-overburden program has been shown to be capable of modelling the airborne EM response of a sphere or dipping plate with optional conductive cover. One limitation is the requirement that the conductive overburden be thin, so if it is too thick, then the early time fit to the data will be poor. The other limitation is if the overburden parameters vary along the profile, the response fit will also be poor. This was evident at Forrestania, where the program was unable to accurately fit the response on either side of the IR2 anomaly.

The software in its current state offers some versatility, ease of use and rapid calculation times. There exists opportunity for future work on the sphere-overburden program to further improve its range of applications and performance. Additional modelling exercises in different geological settings would be useful to further access the programs ability to model airborne EM data in different environments, the Bull Creek deposit in southeast Australia could be a potential deposit for use in a modelling exercise due to the conductive overburden in the area being reasonably representative of that which could be modelled with the sphere-overburden model. Finally, there are some additional options that could feasibly be added to the program to increase its range of uses. For example, 1D inversion along a profile is one such application that could be implemented in the software, another potential feature could be stitched forward models which merge separate sections along a profile to attempt to compensate for the sphere-overburden routines constant overburden assumption. These features if successfully implemented might improve people's ability to use the program for interpretation.

The modelling work done involved exporting the model response and then comparing the field and model data in a separate application. The modelling process could be improved if the field data could be imported into the program and displayed on the same profile as the model data. Another improvement would be to add an inversion algorithm to the package so the program could automatically adjust the model parameters to achieve a good fit. With EM data this normally requires a starting model with a model response reasonably close to the field data.

6.1 Conclusions

We have developed a simple EM forward modelling program that is capable of calculating the EM response of a sphere or dipping-sphere in a resistive host when buried below an overlying thin conductive overburden. The program has distinct advantages over other discrete conductor models such as, ease of use and an efficient run time. Generally, the response calculations are completed in a few seconds after changing parameters. The immediacy of results is of great benefit as a user can specify an orebody of exploration interest and see if the modeled EM response might be observable on a survey. If not, they can change the parameters of the survey (e.g. the base frequency or pulse width) and see if this might result in a stronger more observable response. If it is not possible to detect the target, then the survey might not be worthwhile undertaking. This type of “what if” modelling might also allow the user to determine to what depth orebodies of certain size could be detected below conductive overburden of varying conductance. The program is also of use in an educational setting, it has been successfully incorporated in geophysics classes, where it has proved to be a convenient tool for students to see the change in the decay and shape of the response that might occur when the survey and model parameters are changed.

For example, the students can see how changing the dip and depth and strike orientation changes the EM response. The newly developed sphere-overburden program is consistent with published synthetic examples and able to model real airborne EM data from the Forrestania test site in a manner that is comparable to previously published results. The modelled response directly over the IR2 body is reasonable; however, it has limited ability to model overburdens with variable overburden thickness and conductivity. With further development, additional features and improvements versatility and usefulness could be improved.

References

Dentith, M. C., and Mudge, S. T., 2018, *Geophysics for the mineral exploration geoscientist*: Cambridge University Press.

Desmarais, J. K., and Smith, R. S., 2015a, Survey design to maximize the volume of exploration of the InfiniTEM system when looking for discrete targets: *Journal of Applied Geophysics*, 115, 11–23, DOI: 10.1016/j. jappgeo.2015.02.012.

Desmarais, J.K., and Smith, R. S., 2015b, Decomposing the electromagnetic response of magnetic dipoles to determine the geometric parameters of a dipole conductor: *Exploration Geophysics*, 47, 13–23. <http://dx.doi.org/10.1071/EG14070>

Desmarais, J. K., and Smith, R. S., 2016, Approximate semianalytical solutions for the electromagnetic response of a dipping-sphere interacting with conductive overburden: *Geophysics*, 81(4). DOI: 10.1190/geo2015-0597.1

Dyck, A. V., Bloor, M., and Vallée, M. A., 1980, User manual for programs PLATE and SPHERE: *Research in Applied Geophysics*, 14, University of Toronto Geophysics Laboratory.

Gilgallon, K., Tomlinson, A., and Mortimer, R., 2019, The Forrestania and Nepean electromagnetic test ranges, Western Australia – a comparison of airborne systems: *ASEG Extended Abstracts*, 2019(1), 1–4. DOI: 10.1080/22020586.2019.12073208

Grant, F. S., and West, G. F., 1965, Interpretation theory in applied geophysics. New York: 33 McGraw-Hill.

Hodges, G., Chen, T.-Y. and van Buren, R., 2016, HELITEM® detects the Lalor VMS deposit: *Exploration Geophysics*, 47(4), 285-289, DOI: 10.1071/EG16006

Legault, J. M., Fisk, K., and Fontura, C., 2010, Case study of ZTEM airborne tipper AFMAG results over a magmatic nickel deposit at Forrestania, West Australia, Conference Proceedings, IV Simpósio Brasileiro de Geofísica, Nov 2010, cp-197-00209
DOI: https://doi.org/10.3997/2214-4609-pdb.197.SBGF_2476

Liu, G., and Asten, M. W., 1993, Fast approximate solutions of transient EM response to a target buried beneath a conductive overburden: *Geophysics*, 58, 810–817, DOI: 10.1190/1.1443466.

Prichard, H. M., Fisher, P. C., McDonald, I., Knight, R. D., Sharp, D. R., and Williams, J. P., 2013, The Distribution of PGE and the Role of Arsenic as a Collector of PGE in the Spotted Quoll Nickel Ore Deposit in the Forrestania Greenstone Belt, Western Australia: *Economic Geology*, 108(8), 1903–1921. DOI: 10.2113/econgeo.108.8.1903

Raiche, A., Sugeng, F. and Wilson, G., 2007, Practical 3D EM inversion – the P223F software suite: *ASEG Extended Abstracts*, 1-5, DOI: 10.1071/ASEG2007ab114

Ren, X., Macnae, J., and Hennessy, L., 2019, Three conductivity modelling algorithms and 34 three 3D inversions of the Forrester test site AEM anomaly: *Exploration Geophysics*, 51(1), 14–24. DOI: 10.1080/08123985.2018.1552072

Slattery, S.R. and Andriashek, L.D., 2012, Overview of airborne-electromagnetic and -magnetic geophysical data collection using the GEOTEM survey north of Calgary, Alberta; Energy Resources Conservation Board, ERCB/AGS Open File Report 2012-09, 168 p.

Smith, R. S., and Lee, T. J., 2001, The impulse-response moments of a conductive sphere in a uniform field, a versatile and efficient electromagnetic model: *Exploration Geophysics*, 32, 113–118, DOI: 10.1071/EG01113.

Smith, R.S. and Salem, A. S., 2007, A discrete conductor transformation of airborne electromagnetic data: *Near Surface Geophysics*, 5, 87-95. <https://doi.org/10.3997/1873-0604.2006021>

Smith, R.S., and Wasylechko, R., 2012, Sensitivity cross-sections in airborne electromagnetic methods using discrete conductors: *Exploration Geophysics*, 43, 95-103. <https://doi.org/10.1071/EG11048>

Sørensen, K. I., and Auken, E., 2003, SkyTEM - new development in high-resolution airborne TEM: 9th EAGE/EEGS Meeting. DOI: 10.3997/2214-4609.201414517

Telford, W. M., Geldart, L. P., and Sheriff, R. E., 1990, *Applied Geophysics*. DOI: 10.1017/cbo9781139167932

Vallée, M. A., 2015, New developments in AEM discrete conductor modelling and inversion: 35
Exploration Geophysics, 46, 97–111, DOI: 10.1071/ EG14025.

Huebener, R. (2014). Conductors, semiconductors, superconductors. Heidelberg: Springer.

Abstract

Electromagnetic geophysical methods are used in mineral exploration to detect conductors at depth. In igneous and metamorphic settings, the background half-space is often largely resistive. In such cases, it is important to consider the interaction between the target conductor and any thin, conductive overburden that might exist above the half-space. The overburden is often comprised of glacial tills and clays or the weathering of basement rocks to more conductive material. This situation can be approximated using a discrete conductor model consisting of a “dipping sphere” in a resistive half-space underlying a uniform conductive overburden. A semi-analytical solution that considers the first-order interaction of the sphere and overburden has been derived to calculate the electromagnetic response. The simplicity and efficiency of this solution makes it well suited to be implemented when computation time and immediacy of results are desirable. To this end, we have developed a graphical user interface (GUI) based program to model the electromagnetic response of this model. The program allows users to change the parameters of the survey and target body and quickly view the resulting changes in the shape and decay of the electromagnetic response. The program was tested on airborne electromagnetic data from the Forrestania test range in western Australia. The sphere-overburden model as implemented in the program was able to fit the anomalous data with a spherical body buried 156 m deep and having a dip of 35 degrees to the north.

Keywords

Geophysics, airborne electromagnetic, forward model, program

Acknowledgments

Thank you to my supervisor Richard Smith for giving me this opportunity, thank you to all of my friends, family and fellow grad students that helped me over the course of the last couple of years. Thank you to Adam Smiarowski from CGG for providing the geophysical data used in this thesis.

Table of Contents

Thesis committee	ii
Abstract	iii
Acknowledgments.....	iv
Table of Contents	v
List of Tables	vii
List of Figures	viii
Chapter 1	1
1 Electromagnetic geophysics methods.....	1
1.1 EM geophysics theory	2
1.2 Discrete conductor models.....	5
1.3 Research goals.....	6
Chapter 2	8
2 Sphere-Overburden algorithm.....	8
Chapter 3	11
3 Program design.....	11
3.1 Program development.....	14
Chapter 4	15
4 Methods	15
4.1 Synthetic models	16
4.2 Modelling field data	19
4.3 Forrestania test site.....	19
4.4 HELITEM® data.....	21

Chapter 5	24
5 Forrestania modelling results	24
5.1 Comparison to Maxwell model	27
Chapter 6	29
6 Discussion and future work	29
6.1 Conclusions	30
References	32

List of Tables

Table 1: Time windows (in ms) used for the HELITEM® system when acquiring the Forrestania data.....	23
---	----

Table 2: Model parameters used in the modelling of the IR2 conductor response at the Forrestania EM test range using the sphere-overburden program.....	26
---	----

List of Figures

- Figure 1: Helicopter airborne time domain EM survey, transmitter loop emitting primary magnetic field, inducing secondary currents in target body (transmitter on)..... 4
- Figure 2: Figure 2 Helicopter airborne time domain EM survey, secondary magnetic field generated by the induced currents in target body, measured at receiver (transmitter off). The vector n is normal to the plane of the current flow4
- Figure 3: Simplified synthetic model of a sphere underlying conductive overburden showing electromagnetic parameters and body geometry (after Desmarais and Smith, 2016). 7
- Figure 4: A 3D representation of the dipping sphere model derived in Desmarais and Smith, (2016) where current flow is restricted to parallel planes within an anisotropic sphere..... 8
- Figure 5: Simplified flowchart of the semi-analytic sphere overburden solution as it is implemented in the program. 10
- Figure 6: Screenshot of the sphere-overburden program developed in C++ and python, GUI made using the PyQt5 framework..... 11
- Figure 7: GUI for the sphere-overburden modelling program, variables include, first or second order response, conductivity of sphere and overburden, overburden thickness and more..... 12
- Figure 8: The z-component of the electromagnetic response for a sphere, 100 m below surface with a conductivity of 1 S/m and overburden thickness of approximately 0m 16
- Figure 9: The z-component of the electromagnetic response for a sphere, 300 m below surface with a conductivity of 1 S/m and overburden thickness of approximately 0m 17

List of Figures

- Figure 10: The z-component of the electromagnetic response for a sphere, 100 m below surface with a conductivity of 1 S/m and overburden thickness of 20m 17
- Figure 11: The x- component of the electromagnetic response for a sphere at depth 300 m below surface with conductivity of 1 S/m. (a) Fugro result, the spacing between the major ticks is 200 m (x-axis) (b) sphere-overburden implementation. 19
- Figure 12: The x-component of the electromagnetic response for a sphere dipping at 135 degrees, 300 m below surface with a sphere conductivity of 1 S/m. (a) Fugro result, the spacing between the major ticks is 200 m (x-axis) (b) sphere-overburden implementation. 19
- Figure 13: The z-component of the electromagnetic response for a sphere at depth 300 m below surface with a conductivity of 1 S/m. (a) Fugro result, the spacing between the major ticks is 200 m (x-axis) (b) sphere-overburden implementation. 19
- Figure 14: The z-component of the electromagnetic response for a plate dipping at 135 degrees, 300 m below surface with a conductivity of 1 S/m. (a) Fugro result, the spacing between the major ticks is 200 m (x-axis) (b) sphere-overburden implementation..... 19
- Figure 15: HELITEM® B field z-component response (channel 28). Line 1075 indicated by the red line passes over the IR2 conductor..... 20
- Figure 16: HELITEM® transmitter reference waveform. 22
- Figure 17: Line 1075 of the HELITEM® data for time windows (1-30) on a logarithmic scale. The flight line passes over the IR2 conductor near 6416700N. Each profile corresponds to a delay time from 1.65 to 14.26 ms after shut off. Not all time windows at all locations. 23

List of Figures

Figure 18: Line 1075 of the HELITEM® data for time windows (21-29) on a linear scale. The flight line passes over the IR2 conductor near 6416700N. Each profile corresponds to a delay time from 2.58 to 11.46 ms after shut off..... 23

Figure 19: Results of the sphere-overburden modelling (dashed line) over lying the HELITEM® data (solid line) for Line 1075 showing the late time windows (22-29). The flight line passes over the IR2 conductor near 6416700N. 26

Figure 20: Maxwell model data (red) overlying VTEM Max data (black) from Macnae and Hennessy (2019) from flight line 1075 showing the response of the IR2 conductor at the Forrestania test site..... 28

Chapter 1

1 Electromagnetic geophysics methods

Electromagnetic (EM) prospecting is one of the most widely used methods in mineral exploration. The method was originally developed in the early 1900's in the United States, Canada and Scandinavia where it is common to find a large resistivity contrast between conductive bodies at depth and resistive background material, an ideal geologic setting for the detection of conductive bodies with EM methods (Telford et al, 1990). Airborne methods were later developed in the mid 1950's and were widely used to detect conductors over large areas in a more cost and time efficient manner than ground-based EM surveys (Telford et al, 1990). Both ground and airborne EM systems have configurations that differ in terms of system geometry, operating frequency, transmitter waveform and more. The variety of system configurations make different airborne systems uniquely suited for use in different settings, some of the most commonly used airborne systems include HELITEM®, VTEM, MEGATEM, HELISAM and others. Airborne EM systems are also developed for specific applications outside of mineral exploration, an example of this is the airborne EM system SKYTEM, which is widely used in hydrogeological applications for salinity mapping as the high signal-to-noise ratio and fast transmitter shut off allow for collection of high-resolution data in the near surface and an estimate of depth to the target body (Sørensen and Auken, 2004). Active source EM systems consists of a transmitter and receiver coil at or above surface, typically at a constant spacing. In the case of airborne EM the transmitter and receiver coils can be towed behind the aircraft or attached to the extremities of the aircraft for a fixed wing system. The variety of airborne EM systems further adds to the method's versatility and effectiveness as a tool for detecting conductive bodies at depth.

1.1 EM geophysics theory

The practice of EM surveying begins with generation of a primary field that penetrates into the subsurface. For the case of time domain EM methods, the primary field is associated with a bipolar current pulse flowing in a transmitter loop that repeats at a specific base frequency. The current waveforms can have the shape of a half sine-wave, step or ramp (Telford et al, 1990). The changing primary field generates electrical currents termed secondary currents in conductive material in the ground. These currents in turn, have an associated secondary magnetic field that propagates out from the conductive body and is measured at or above surface at the receiver producing a secondary field that generally decays with time (Telford et al, 1990). The secondary field is measured as a function of the delay time (after the transmitter shut off) in measurement intervals termed time windows and are traditionally numbered from early to late time. The amplitude and decay rate of the secondary field measured at the receiver provides information about contrasting physical properties of the subsurface, this contrast in physical properties allows us to detect conductive bodies at depth and make geological interpretations of the subsurface. Figures 1 & 2 depict the processes of EM induction that occurs in the subsurface during an airborne time-domain survey over a conductive body. Electromagnetic induction processes are governed by the Maxwell equations (Grant and West, 1965). A current driven through a transmitter (figure 1) has an associated primary magnetic field (Ampere's law). The current switches off after the transmitter pulse, this results in a time-varying magnetic field in the subsurface, which according to Faraday's law results in an electric field circulating around the primary magnetic field. If there is conductive material in the subsurface, then Ohm's law tells us that this electric field is proportional to an induced current flow within the conductive body. Ampere's law applied to the induced (secondary) current gives a secondary magnetic field (figure 2) that can be sensed at the receiver, typically during the transmitter off-time. The resolving power and overall success of any given EM geophysics survey is dependent upon how

the physical properties of the target vary from that of the background material. The physical properties of greatest relevance to EM methods are as follows (in order of importance): 1) electrical conductivity 2) magnetic permeability 3) dielectric permittivity (Telford et al, 1990). These physical properties will determine the time-decay curve of the secondary field measured at the receiver where, conductive bodies will have a slower secondary field decay rate. It is important to consider factors that impact conductivity and resistivity in the subsurface. The main factors that control electrical conductivity of the subsurface are; mineralogy, porosity and pore saturation. The electrical current within a rock will travel along the path of least resistance: in ore-bearing rocks the current will travel through any of the metal-oxides, metal-sulfides, native metals or any graphite present in the rock, avoiding the relatively resistive silicate minerals. Current can flow through these substances with little resistance as the outer electrons of the atoms that make up the materials are loosely bound and can move freely (Huebener, R., 2014). The magnetic permeability of geological environments has been shown to impact the response of EM surveys and must be accounted for when the target body has a high concentration of magnetite and pyrrhotite, which have very high magnetic permeabilities. The dielectric permittivity of a material is the ability of a given substance to hold an electric charge. In electromagnetic prospecting methods, the dielectric permittivity is assumed to be negligible, which is called the *quasi-static* assumption (Grant and West, 1965) These physical contrasts along with other properties such as depth to body, shape and orientation will determine if the EM survey is able to detect the target conductor. The results of an EM survey are interpreted by comparing the measured response over a profile to the calculated response of forward models consisting of various simple shapes with specific properties. Common configurations include a conductive sphere in a uniform or dipole field (Grant and West, 1965), or a plate (Dyck et al., 1980). Simple forward models are not always appropriate for responses measured in field surveying, it is therefore desirable to generate forward models that are representative of field

data settings, in terms of the stratigraphy and orientation of the underlying geology and its associated physical properties.

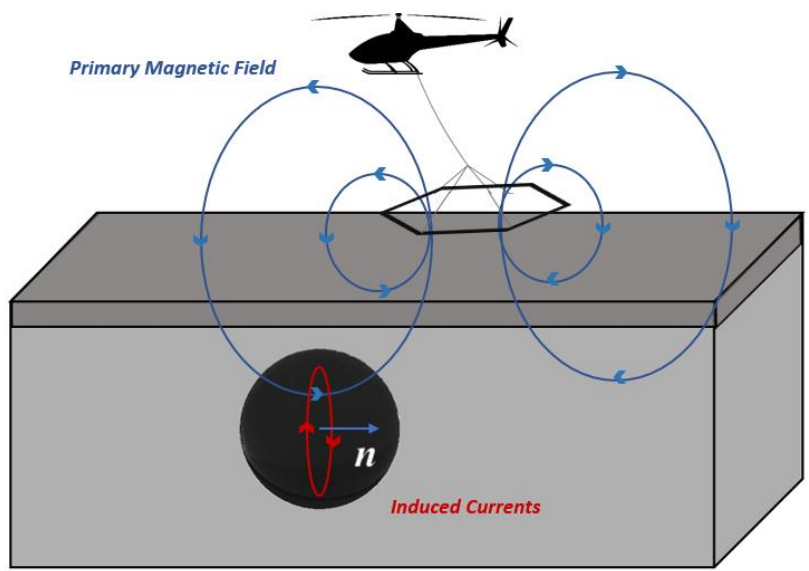


Figure 1: Helicopter airborne time domain EM survey, transmitter loop emitting primary magnetic field, inducing secondary currents in target body (transmitter on). The vector n is normal to the plane of the current flow

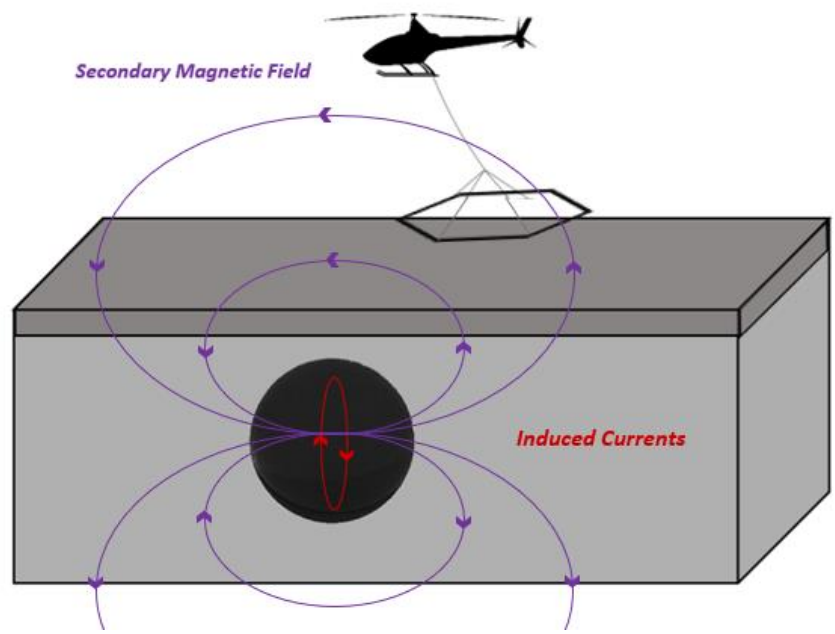


Figure 2: Helicopter airborne time domain EM survey, secondary magnetic field generated by the induced currents in target body, measured at receiver (transmitter off).

1.2 Discrete conductor models

Discrete conductor models in mineral exploration geophysics are useful for gaining an understanding of the response of highly conductive target bodies and can be used for the interpretation of airborne, ground or borehole EM data. For EM methods, the discrete target bodies in these forward models are most commonly represented as plate-like or spherical conductors (Lamontagne et al., 1988). It is possible to infer information about the parameters of the target body by fitting a discrete conductor model to acquired data or by directly analyzing the shape and decay of the EM response (Valleé, 2015), which is commonly used in the processing of airborne EM data. Plate models are most commonly used, as they are useful for representing thin and dipping conductors; however, for thicker, discrete conductors, sphere models are more appropriate, as the current can flow in multiple orientations perpendicular to the primary field (Dentith and Mudge, 2014). The mathematical formulations for discrete models in half-spaces and below overburdens (Raiche et al., 2007) can be complex and relatively computationally expensive. Hence, they have not been implemented into programs that can be used for interactively modelling EM responses.

The EM response of a small sphere in a uniform field (Grant and West, 1965) was adapted by Smith and Lee (2001) to model both sphere like bodies and spheres where the currents are constrained to flow in a plane with a specified strike and dip. The latter variant is able to mimic the response of dipping plates. This versatile model has been used for interpreting airborne EM data (Smith and Salem, 2007; Desmarais and Smith, 2015a) and determining the cross-sections of investigation associated with specific EM systems (Smith and Wasylechko, 2012; Desmarais and Smith, 2015b).

1.3 Research goals

In mining geophysics, we are often interested in the case of a discrete conductor embedded in a resistive environment or half-space. This situation is common in the Canadian shield, where conductive massive sulfide orebodies are embedded in resistive metamorphic or igneous rocks. If there is a conductive overburden above this resistive half-space, then it is important to account for the interaction between the discrete conductor and the upper layer of conductive overburden (Desmarais and Smith, 2016). A simplified model for the case of a sphere underlying conductive overburden is shown in figure 3. A semi-analytical solution for this model was derived in Desmarais and Smith (2016) and is implemented in our modelling software. The program can quickly generate the airborne EM response for synthetic models such as the model presented in figure 1. In normal sphere solutions, the EM current flow is perpendicular to the vector \mathbf{n} , which is parallel to the time-varying magnetic field exciting the sphere. However, the response of plate-like bodies can also be approximated by specifying that the induced current can only flow at a specific orientation. This is what would occur if the sphere was comprised of multiple thin layers with alternating conductive and resistive material. Such a sphere is essentially anisotropic, with current only being able to flow in the plane of the conductive layers and not in the perpendicular direction. For brevity, we call this model a “dipping sphere”. A 3D representation of this model is presented in figure 4 where the induced currents flow within parallel planes, in this case slightly off vertical. The ability of this model to be representative of a plate-like or spherical body interacting with conductive overburden makes it a uniquely versatile model (Smith and Lee, 2001).

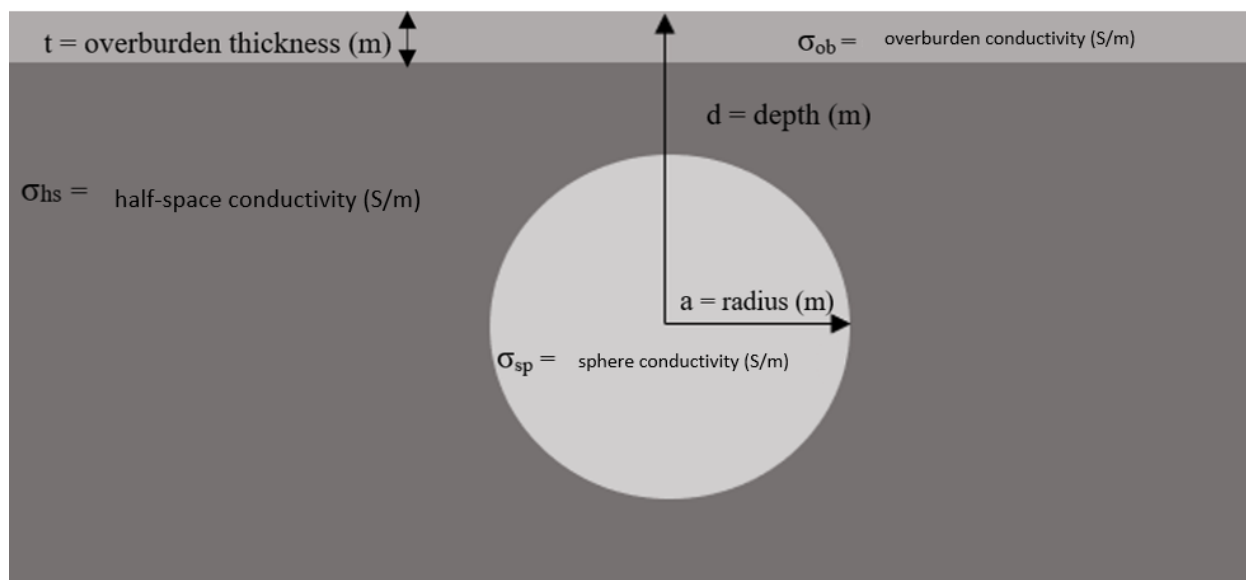


Figure 3: Simplified synthetic model of a sphere underlying conductive overburden showing electromagnetic parameters and body geometry (after Desmarais and Smith, 2016).

The response of the dipping sphere buried below overburden can be calculated in a few seconds on a laptop computer. This provided us with an opportunity to create an interactive computer program that could be used for multiple purposes:

- 1) for students to learn how the EM response varies when various parameters of the model, e.g. dip, depth, overburden conductivity;
- 2) for geophysicists to test whether the response of an expected target would be evident above the response of the overburden or the noise levels; and
- 3) for geophysicists to adjust the acquisition parameters, such as the base frequency to a system so that their target could be identified on an EM survey.
- 4) For geophysicist to explain a measured response by adjusting the parameters of the model until the model response is similar to the measured response.

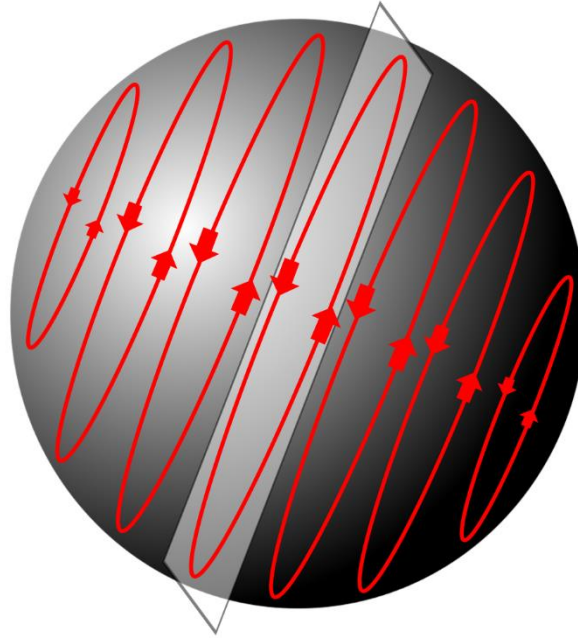


Figure 4: A 3D representation of the dipping sphere model derived in Desmarais and Smith, (2016) where current flow is restricted to parallel planes within an anisotropic sphere.

Chapter 2

2 Sphere-Overburden algorithm

The semi-analytic solution of Desmarais and Smith (2016) assumes that the combined response of the sphere and overburden is reasonably approximated by a sphere excited by the currents induced in the overburden. This approximation was proposed in Liu and Asten (1993) using the estimated response of a wire loop interacting with conductive overburden. They argued that the response may be written as the overburden field H_{ob} plus a sum of terms H_n accounting for the inductive interaction between the sphere and overburden.

$$H = H_{ob} + \sum_{n=1}^{\infty} (H_n)$$

Liu and Asten (1993) demonstrated that using only the first-order term

$$H \approx H_{ob} + H_1$$

gave a reasonable approximation as the magnitude of the higher-order terms (H_2 , H_3 , etc) are progressively weaker. The first-order term assumes that the sphere response is excited by the secondary field of the currents induced in the overburden. The sphere-overburden algorithm also assumes that the sphere is not in contact with the overburden, so there is no channeling of overburden currents into the sphere. The formulation also assumes that the sphere is a dipole in a uniform field, which Smith and Lee (2001) argued was reasonable for the airborne EM configuration, where the transmitter and receiver are normally a large distance from the target. These approximations greatly reduce computation time as the response at each location may be calculated by convolving the overburden response with that of the target, which is a sum of decaying exponentials (Desmarais and Smith, 2016). The short computation time will allow many electromagnetic responses to be generated along a profile quickly. Our initial efforts have been to model the response of airborne EM systems with arbitrary waveforms and geometries. The arbitrary waveform is accounted for by a second convolution integral, where the impulse response of the sphere-overburden is convolved with the EM system current waveform. Airborne EM systems generally only have one or two receiver positions for each transmitter dipole location on the profile. However, the program could be adapted for ground EM systems, which generally have one large loop transmitter position and multiple receiver positions (e.g. Desmarais and Smith, 2015b). A simplified flowchart of the response calculations made by the sphere-overburden program is presented below in figure 5.

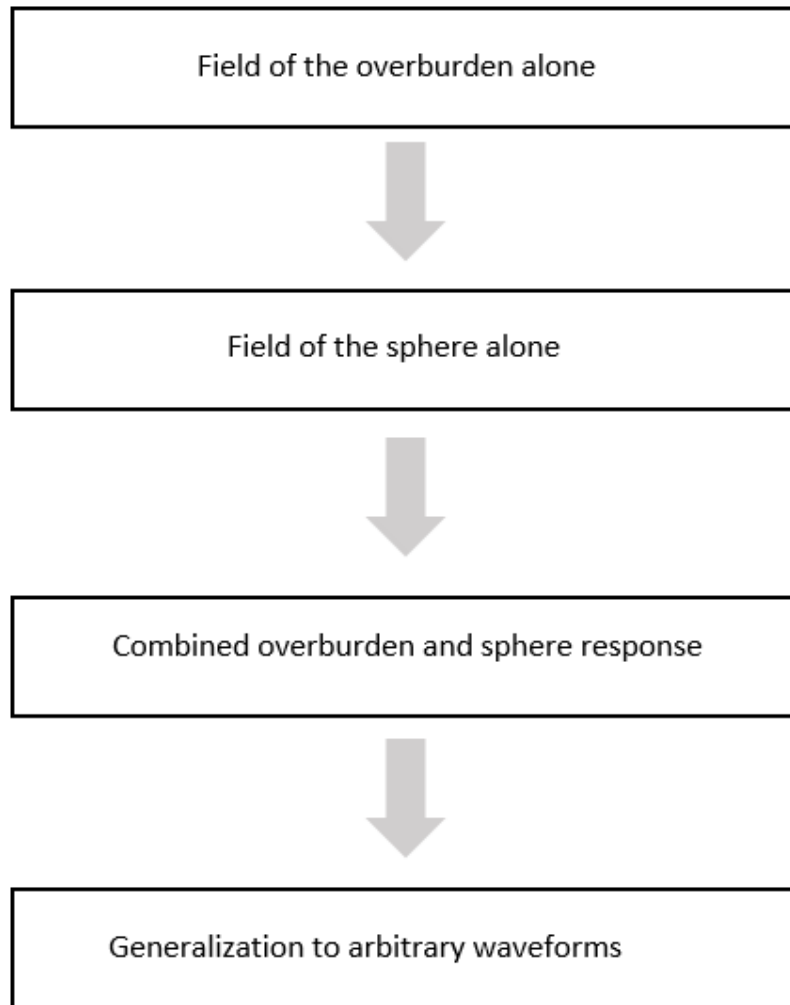


Figure 5: simplified flowchart of the semi-analytic sphere overburden solution as it is implemented in the program.

Chapter 3

3 Program Design

The sphere-overburden program was written in C++ and python, the program was designed to provide a user friendly and fast method of modeling airborne EM responses. A screen capture of the programs graphical user interface (GUI) is presented in figure 6. The screen shot presents the z-component response calculated and plotted on the right-hand side of the image, given the user defined parameters on the options widget on the left-hand side of the screen.

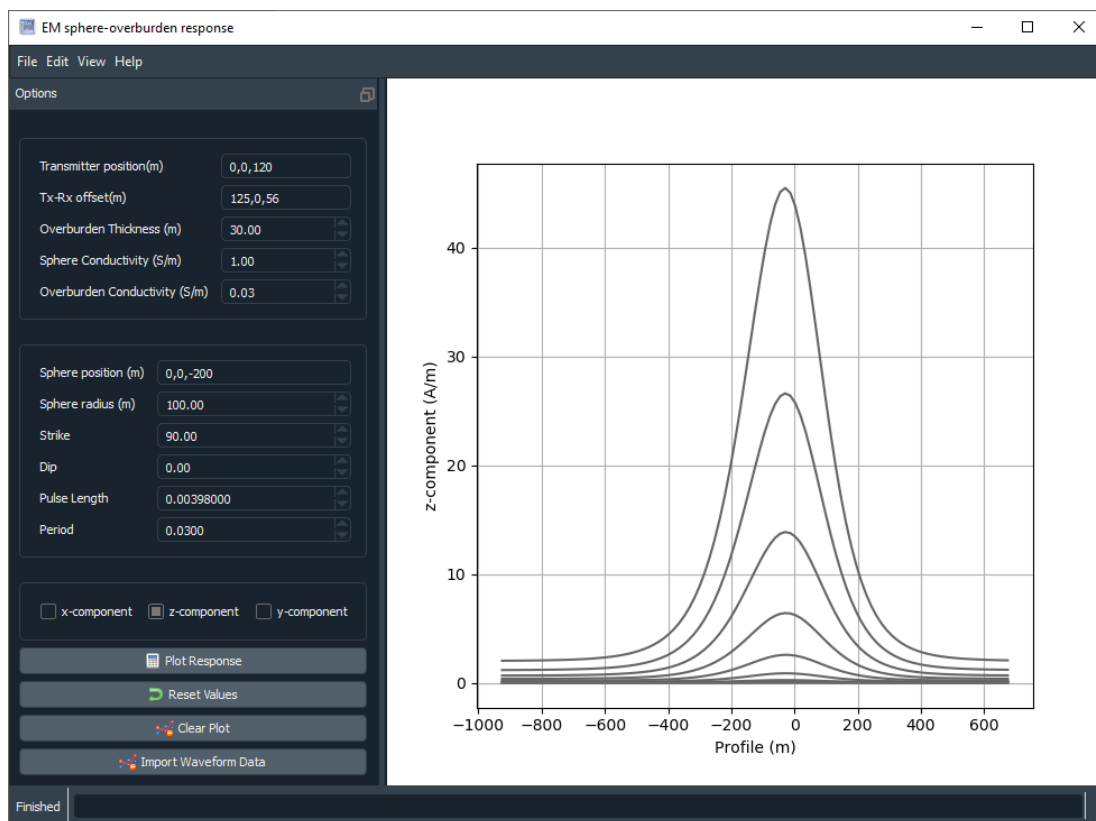


Figure 6: Screenshot of the sphere-overburden program developed in C++ and python, GUI made using the PyQt5 framework

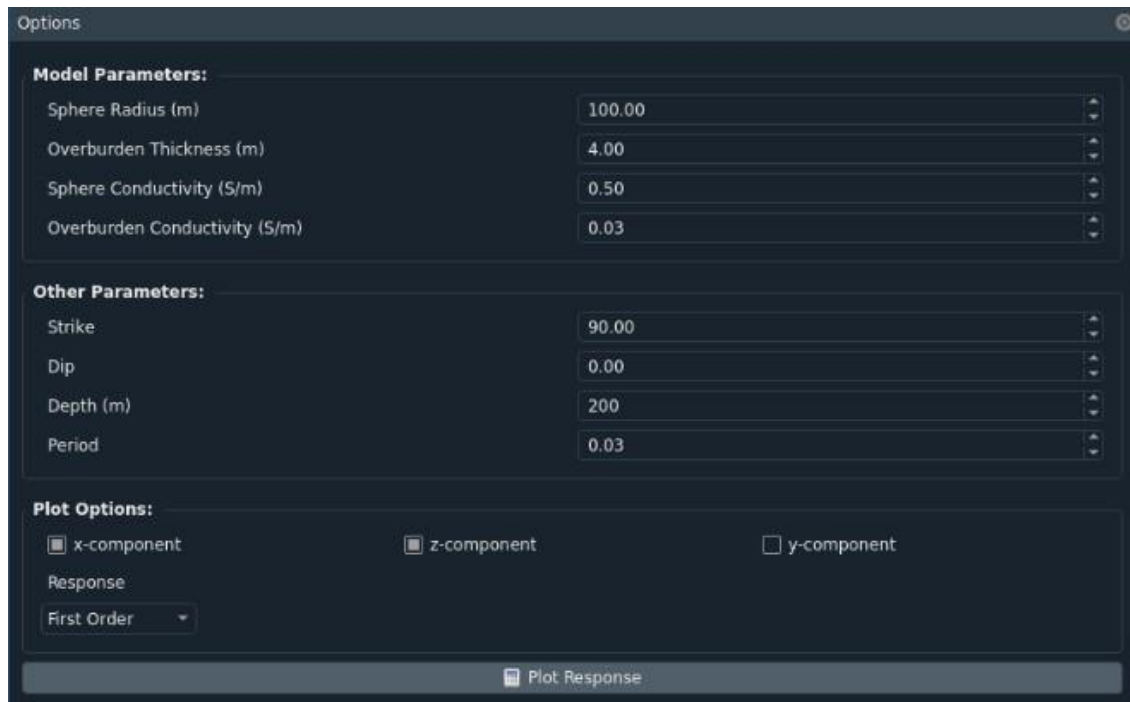


Figure 7: GUI for the sphere-overburden modelling program, variables include, first or second order response, conductivity of sphere and overburden, overburden thickness and more

Figure 7 removes the plotting area from figure 6 to highlight some of the system parameters that can be manually changed by the user using the GUI, including the transmitter position relative to the plotting point, the receiver position, relative to the transmitter. Note that the offsets are assumed to be positive when the receiver is to the left of the transmitter for the x offset, into the page for the y offset and up for the z offset. If negative offsets are used, then the sign of the response may be different from expected as the x component is defined as having a positive response in the direction to the right, but some airborne EM systems define a positive x response as being in the direction from the transmitter to the receiver.

Other variables the user is able to change via the GUI include the sphere radius, conductivity, depth and overburden thickness and conductivity. Note however, that the algorithm assumes a thin-sheet approximation for the overburden (Grand and West, 1965), so entering a greater thickness and correspondingly smaller conductance will give identical results.

The GUI can also be used to specify the survey parameters such as the dip, strike, transmitter dipole moment, transmitter base frequency and profile length. When the dip is specified to be zero then the “dipping sphere” model is not used and the normal sphere models is used, where the currents flow perpendicular to the direction of the excitation field from the currents induced in the overburden. The components of the response to be plotted are selected using the corresponding x, y, z component buttons located underneath the system variables widget, the program allows for multiple components to be plotted at the same time to allow the user to quickly and easily compare between the x,y and z component of the airborne EM response. The function buttons at the bottom left of the GUI presented in figure 7 allow the user to control the functionality of the program including generating the responses, clearing the plots and resetting the parameter values to default. The import waveform button allows to user to import time window data and transmitter current pulse data in the form of a csv file. The corresponding data sets are read into the program and used in the sphere-overburden routine to generate a response for a specific EM system.

3.1 Program development

This user interface was written in python using the PyQt5 framework, parts of the response computation functions were written in C++ to take advantage of the computational efficiency that can be achieved using a programming language that uses a compiler to generate object code. Multiple code libraries and frameworks were used in the development of the sphere-overburden program, the open source C++ library Eigen was used for its linear algebra functionality and Pybind11 was used to wrap the C code in python. The python library Quadpy was used for its implementation of the Gauss-Kronrod numeric integration routine (used for convolution), which offers a large improvement in runtime over standard integration methods. Implementing performance-based libraries and frameworks in the software provides significant performance increases over interpreted languages for scientific or numerical programming. The sphere-overburden code was profiled and compared to an earlier implementation of the sphere-overburden calculations programmed in Matlab, a widely used interpreted language in the science and engineering community. Two EM responses were generated, one response is the impulse response and the second involved convolving the impulse response with a transmitter current pulse defined using a 400-point time series. The C++/python implementation calculated the impulse response in 4 seconds compared to 20 seconds for the Matlab implementation. When convolving with the transmitter waveform data, the C++/python implementation generated a response in 3 minutes while the Matlab implementation completed in 12 minutes. These times are of course machine dependent. The use of optimized open-source libraries and compiled code provides a sphere-overburden solution that is fast and convenient for the end user. All libraries and frameworks used are open source and covered under the MIT license. The program is compiled to a windows executable using the pyinstaller library, this allows for easy distribution of the software.

Chapter 4

4 Methods

Airborne EM data in its raw form can be problematic for inexperienced people to interpret, particularly if they do not have access to geophysics modelling software. Hence, the data will often be processed and converted to data formats that are more readily interpretable such as conductivity depth images (CDI) or perhaps even 2D or 3D inversions. These images and inversions require a starting forward model to produce good results. Simple starting models such as half spaces are sometimes used, but for discrete conductive bodies, the most geologically reasonable results are obtained if the starting model is also a discrete conductor and has a reasonable fit to the data. Hence a simple sphere-overburden model might be a good starting model, even when the actual situation is more complex (not a sphere or not in a resistive host). One way to generate such appropriate models for airborne EM profiles is by fitting the anomalies observed along a flight line using modelling software such as the Maxwell plate modelling software (<http://www.electromag.com.au/maxwell.php>) or the Multiloop modelling package (<https://www.lamontagnegeophysics.com/products-multiloop-home.html>). The sphere-overburden program provides another modelling software package that can easily include conductive overburden and allows the flexibility of spheres and dipping spheres. It is an accessible tool that can be used for fast modelling prior to using more sophisticated tools such as Maxwell or Multiloop, that allow modelling using multiple lines, multiple bodies, etc.

4.1 Synthetic models

The sphere-overburden program is able to generate EM responses over a sphere or dipping plate with user-defined model parameters, these synthetic models allow users to see the resulting changes in the shape and amplitude of the EM response. Figures 8-10 are synthetic sphere models that show the z-component of the EM response for varying sphere depths and overburden thicknesses. Comparing figure 8 and figure 9 it is seen that as the sphere depth is increased from 100 m to 300 m the amplitude of the response decreases and the peak of the anomaly becomes more broad, there is no overburden response as the thickness of the overburden in these models is set to be a negligible thickness. Comparing figure 8 to figure 10 it is observed that when an overburden is introduced to the model the early-time channels increase in amplitude; this is most evident on either side of the sphere.

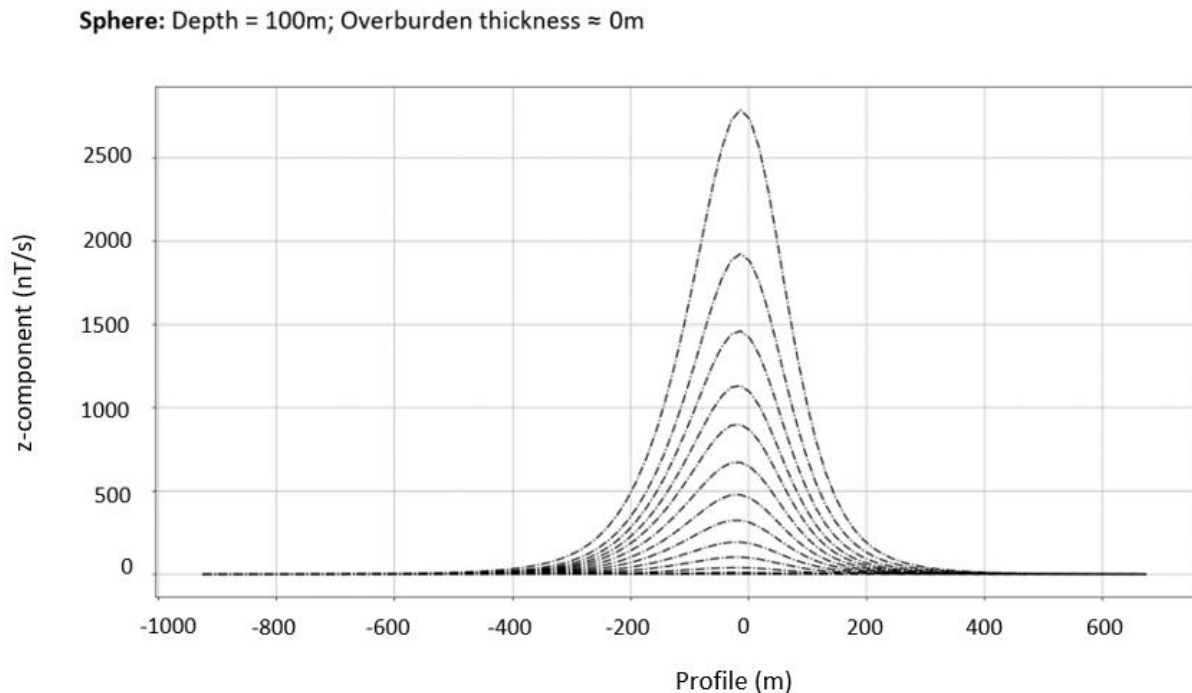


Figure 8: The z-component of the electromagnetic response for a sphere, 100 m below surface with a conductivity of 1 S/m and overburden thickness of essentially 0 m

Sphere: Depth = 300m; Overburden thickness \approx 0m

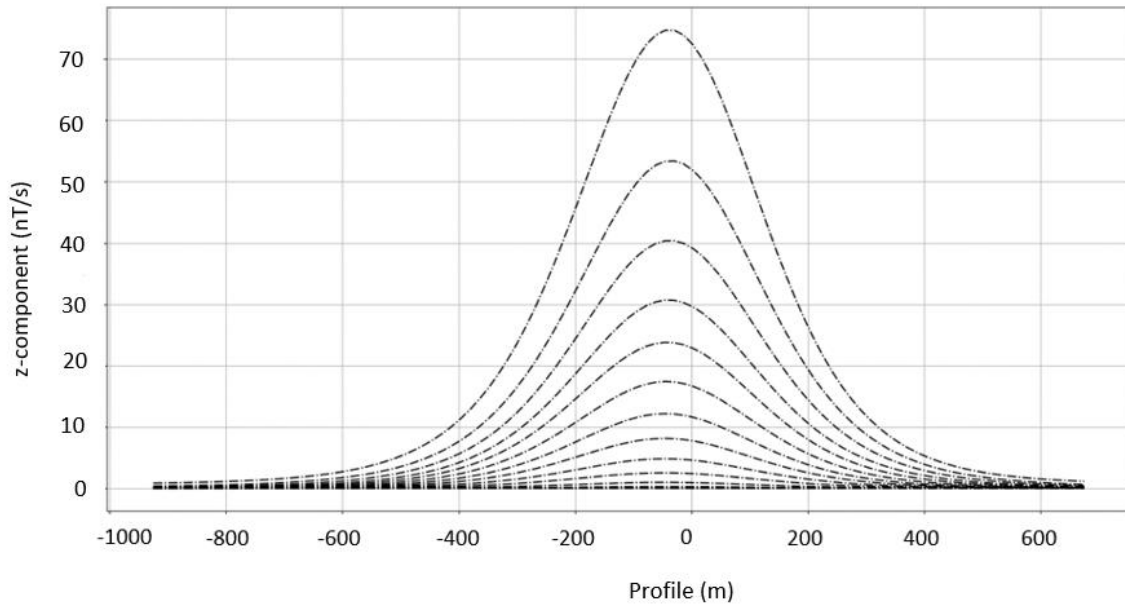


Figure 9: The z-component of the electromagnetic response for a sphere, 300 m below surface with a conductivity of 1 S/m and overburden thickness of essentially 0 m

Sphere: Depth = 100m; Overburden thickness = 20m

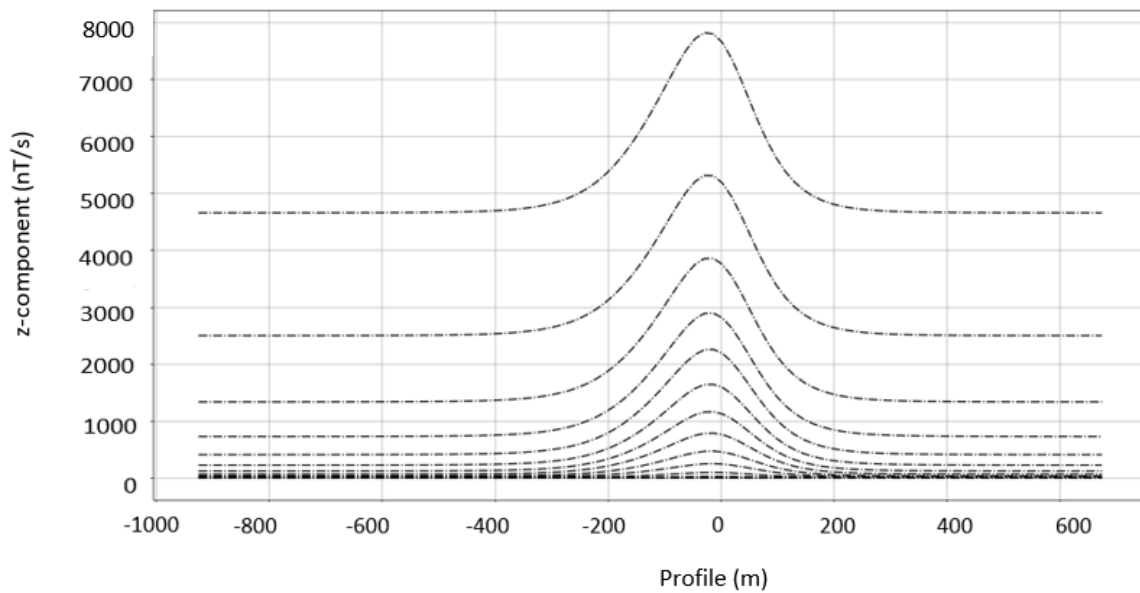


Figure 10: The z-component of the electromagnetic response for a sphere, 100 m below surface with a conductivity of 1 S/m and overburden thickness of 20 m

To validate the EM responses generated by our program, we compare the results of the program with synthetic models generated by Fugro and presented in Slattery and Andriashok (2012), for both a sphere model and a dipping-sphere model. The synthetic models were presented as part of a 2012 open file report describing airborne EM and magnetic data collection using the GEOTEM system in Alberta. The synthetic models presented in the report were generated using the sphere in a uniform field algorithm derived in Smith and Lee, (2001), but adapted to the time domain, using the formulation of Smith and Neil (2013). The x- and z-components of the response for a sphere and dipping-sphere in free space with no conductive overburden as presented in Slattery and Andriashok (2012) are shown in figures 11-14 (a). The response generated by our implementation are shown in figures 11-14 (b). Figures 11 and 12 are for the x-component, figures 13 and 14 are for the z-component. It is seen that for both, the case of the dipping-sphere and sphere model, the shape of the response in the x- and z-components produced by our program is in agreement with those of Slattery and Andriashok (2012). The amplitude of the plots is not expected to be in agreement due to uncertainty in system parameters, the dipole moment and sphere radius used to generate the Fugro responses were not specified in Slattery and Andriashok (2012). Additionally, the EM responses generated by Fugro used a sphere model which has no conductive cover, to compensate for this the overburden thickness parameter of the sphere-overburden algorithm is set to be a negligible thickness. There is some discrepancy in the amplitude of the responses, overall, this comparison confirms that key aspect of the sphere-overburden program have been implemented correctly, further validation efforts using more representative models would be beneficial.

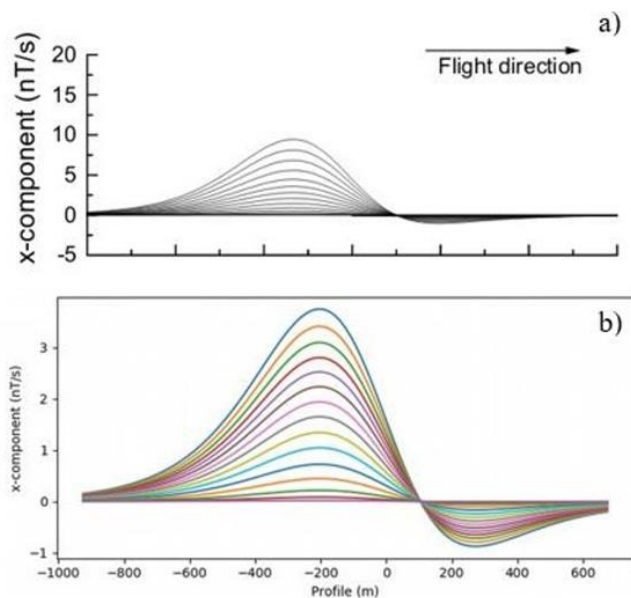


Figure 11: The x- component of the electromagnetic response for a sphere at depth 300 m below surface with conductivity of 1 S/m. (a) Fugro result, the spacing between the major ticks (x-axis) is 200 m (b) This implementation.

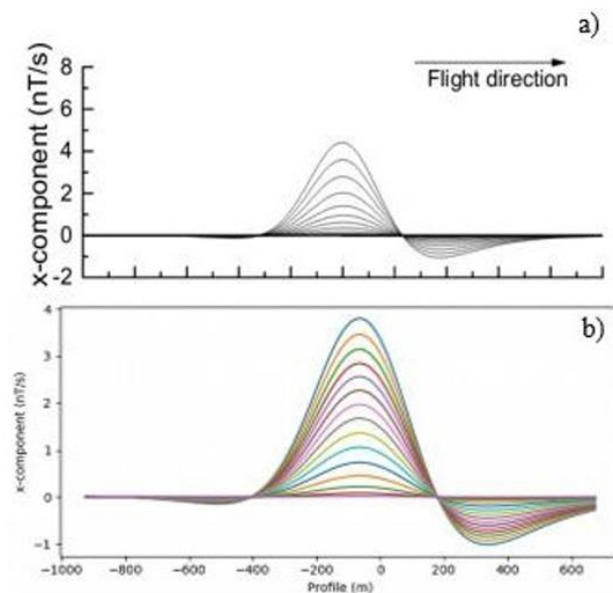


Figure 12: The x-component of the electromagnetic response for a sphere dipping at 135 degrees, 300 m below surface with a sphere conductivity of 1 S/m. (a) Fugro result, the spacing between the major ticks (x-axis) is 200 m (b) This implementation.

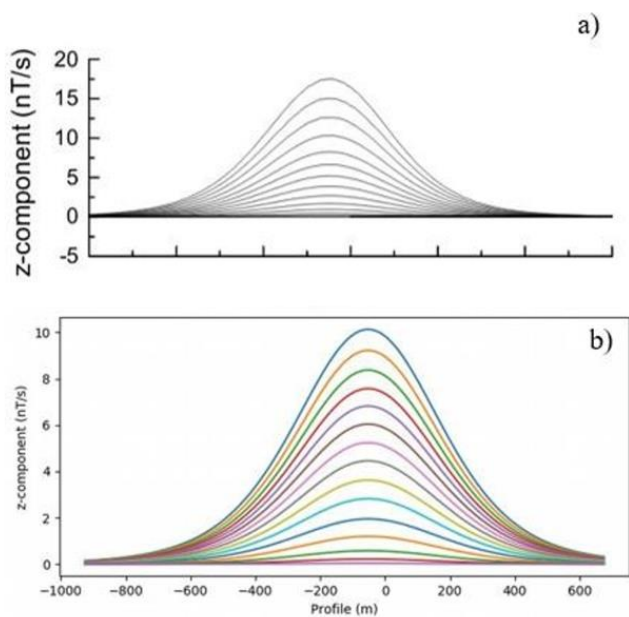


Figure 13: The z-component of the electromagnetic response for a sphere at depth 300 m below surface with a conductivity of 1 S/m. (a) Fugro result, the spacing between the major ticks (x-axis) is 200 m (b) This implementation.

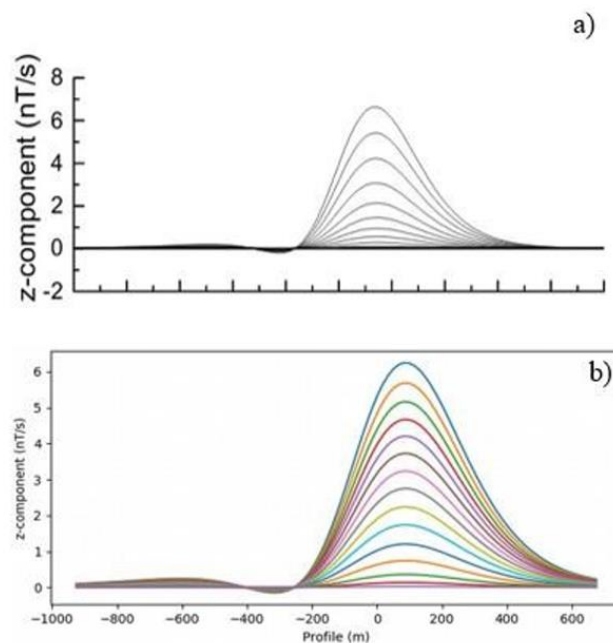


Figure 14: The z-component of the electromagnetic response for a plate dipping at 135 degrees, 300 m below surface with a conductivity of 1 S/m. (a) Fugro result, the spacing between the major ticks (x-axis) is 200 m (b) This implementation.

4.2 Modelling field data

In the *Research goals* section, four reasons were enumerated for developing the program. It is fairly straight forward to imagine how the program would be used to achieve the first three goals. Users can adjust the parameters of the bodies and the EM acquisition system in the GUI in order to observe the changes in the response profiles and how the calculated amplitudes compare with those of the overburden response and the noise levels. In this section we show how the newly developed sphere-overburden program, can be used to achieve the fourth goal, of modelling field data recorded over a known anomaly. The airborne data set was selected based on two main criteria. Firstly, the survey target should include a well constrained, well defined conductor that has been identified using multiple EM systems. Secondly, the survey area should have a regional geology that is representative of a discrete target with an underlying conductive overburden.

4.3 Forrestania test site

The Forrestania site includes a group of Ni-Cu deposits located approximately 400 km east of Perth in Western Australia (Prichard et al, 2013). Test ranges such as Forrestania present an opportunity for objective comparison and assessment of multiple types of airborne EM systems and their different specifications and system geometry (Gilgallon et al, 2019). The Forrestania test range is located on open, readily accessible land making it an ideal location for ground, airborne and borehole EM surveys, and hence, there has been numerous EM surveys and drilling carried out on the test site resulting in well-defined conductors and geology in the area with associated ground truth (Gilgallon et al, 2019). One of the surveys flown over the Forrestania EM test range was completed using the HELITEM® time domain airborne system.

Figure 15 presents HELITEM® B field z-component (dB/dt) data that has been collected over Forrestania and gridded. The red line shown in figure 15 depicts the flight line 1075 which passes over the IR2 conductor. The HELITEM® system is able to detect the response due to the shallow IR2 conductive body, the survey was also able to measure the response of more conductive material to the north of the IR2 conductor that is attributed to conductive overburden.

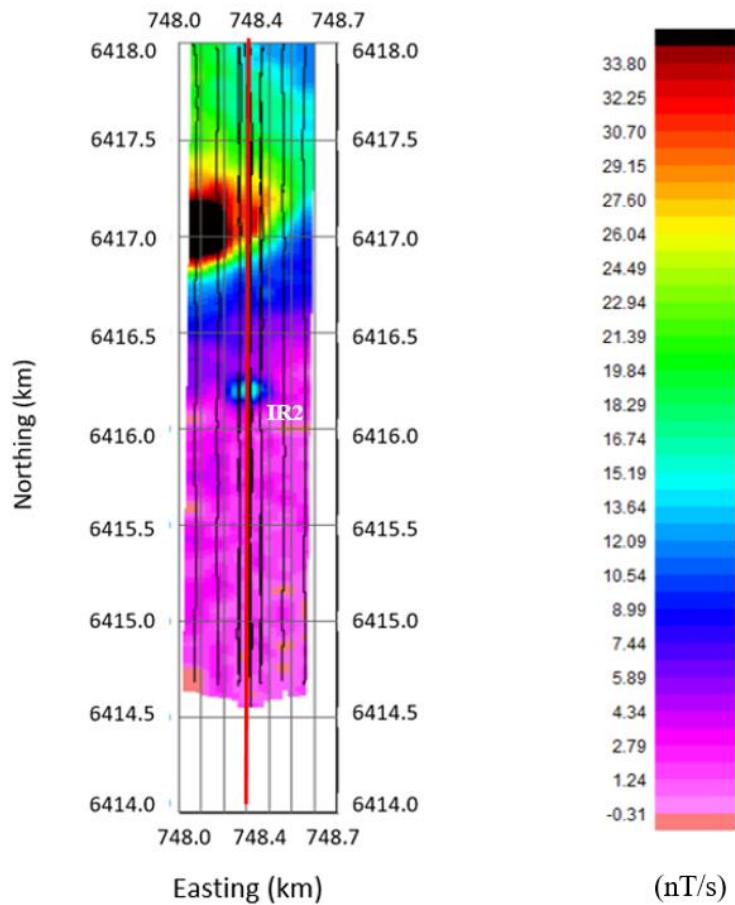


Figure 15: HELITEM® B field z-component response (channel 28). Line 1075 indicated by the red line passes over the IR2 conductor.

4.4 HELITEM® data

HELITEM® data collected over the Forrestania test site was provided by CCG for use in this modelling exercise. The HELITEM® system is an airborne time-domain EM system often used in environmental and mineral exploration applications (Hodges et al, 2016). The data set consist of 11 flight lines of 30 windows (listed in Table 1) measuring dB/dt. For this survey, the HELITEM® system was operating at a base frequency of 25 Hz with a sampling frequency of 102400 Hz, the transmitter current pulse is plotted in figure 16. Flight line 1075 of the HELITEM® data set was chosen for modelling the response over the IR2 conductor using the sphere-overburden program. Figure 17 shows the z-component profile on a log scale with the anomaly associated with the IR2 conductor evident at 6416700N. The data is first plotted on a log scale where all windows can be seen at once, so the conductor response can be seen in the context of the large overburden response at early time. The relative strength of the conductor anomaly relative to the overburden is greatest in the late time windows with increasing noise becoming evident in the very late windows. Hence, we model the late time windows (21 to 29) when trying to explain the response of the IR2 conductor with the sphere-overburden program. These windows can be seen on figure 18, where the response of the IR2 conductor is evident in the context of a rapid rise in amplitude to the north, attributed to conductive overburden. To generate a model to fit the HELITEM® data, we use the ‘read in waveform’ feature of the sphere-overburden program to import the reference HELITEM® waveform data, and the time windows in csv format. The transmitter reference waveform is convolved with the impulse response to generate the model response as described in Desmarais and Smith (2016).

HELITEM® window mid-times (ms)		
Ch 1-4 – on time data	Ch 13 – 0.605	Ch 22 – 3.10
Ch 5 – 0.165	Ch 14 – 0.725	Ch 23 – 3.73
Ch 6 – 0.195	Ch 15 – 0.865	Ch 24 – 4.50
Ch 7 – 0.225	Ch 16 – 1.035	Ch 25 – 5.42
Ch 8 – 0.260	Ch 17 – 1.235	Ch 26 – 6.53
Ch 9 – 0.305	Ch 18 – 1.480	Ch 27 – 7.88
Ch 10 – 0.360	Ch 19 – 1.785	Ch 28 – 9.50
Ch 11 – 0.425	Ch 20 – 2.145	Ch 29 – 11.46
Ch 12 – 0.505	Ch 21 – 2.580	Ch 30 – 14.26

Table 1: Time windows (in ms) used for the HELITEM® system when acquiring the Forrestania data

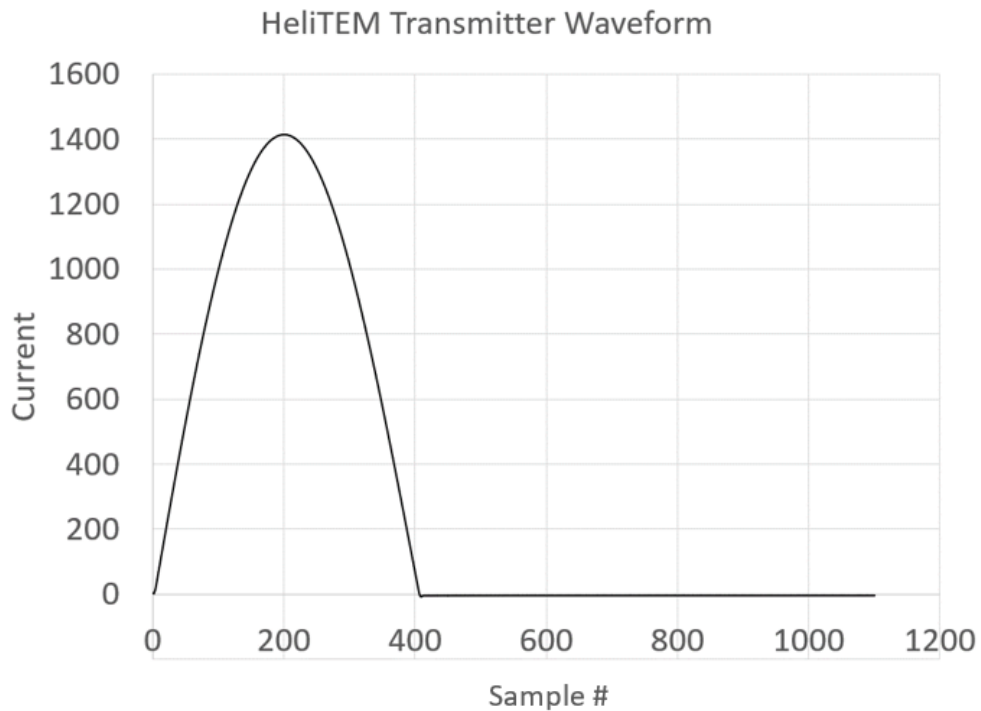


Figure 16: HELITEM® transmitter reference waveform.

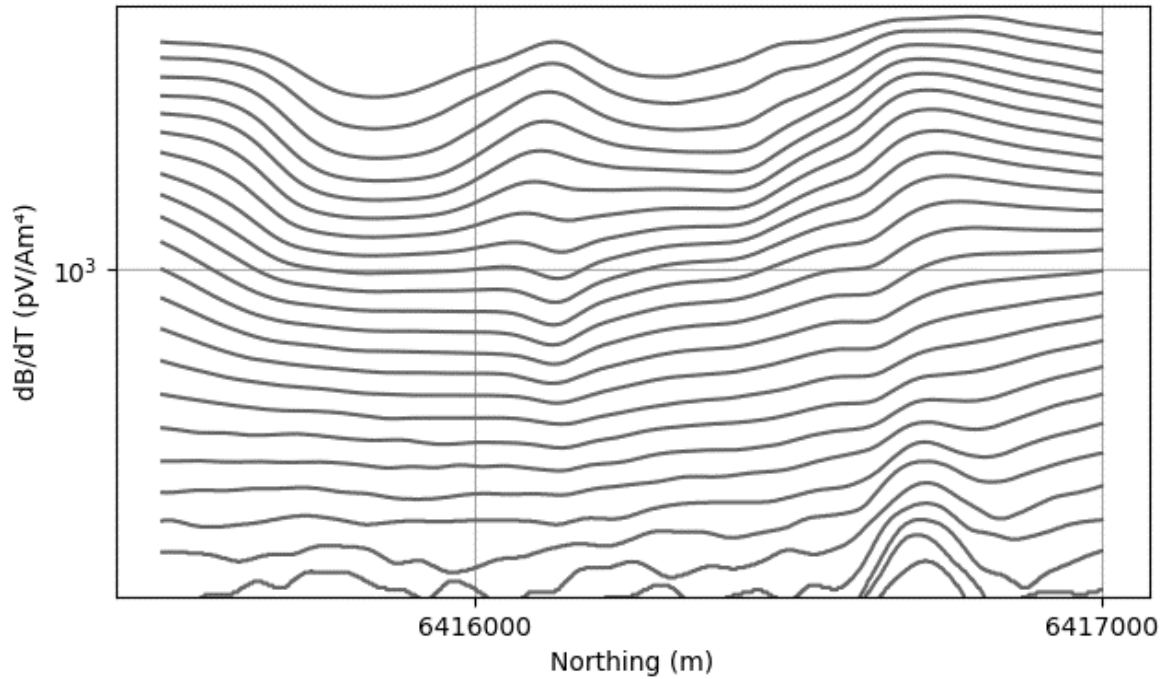


Figure 17: Line 1075 of the HELITEM® data for time windows (1-30) on a logarithmic scale. The flight line passes over the IR2 conductor near 6416700N. Each profile corresponds to a delay time from 0.165 to 14.26 ms after shut off. Not all time windows are evident at all locations.

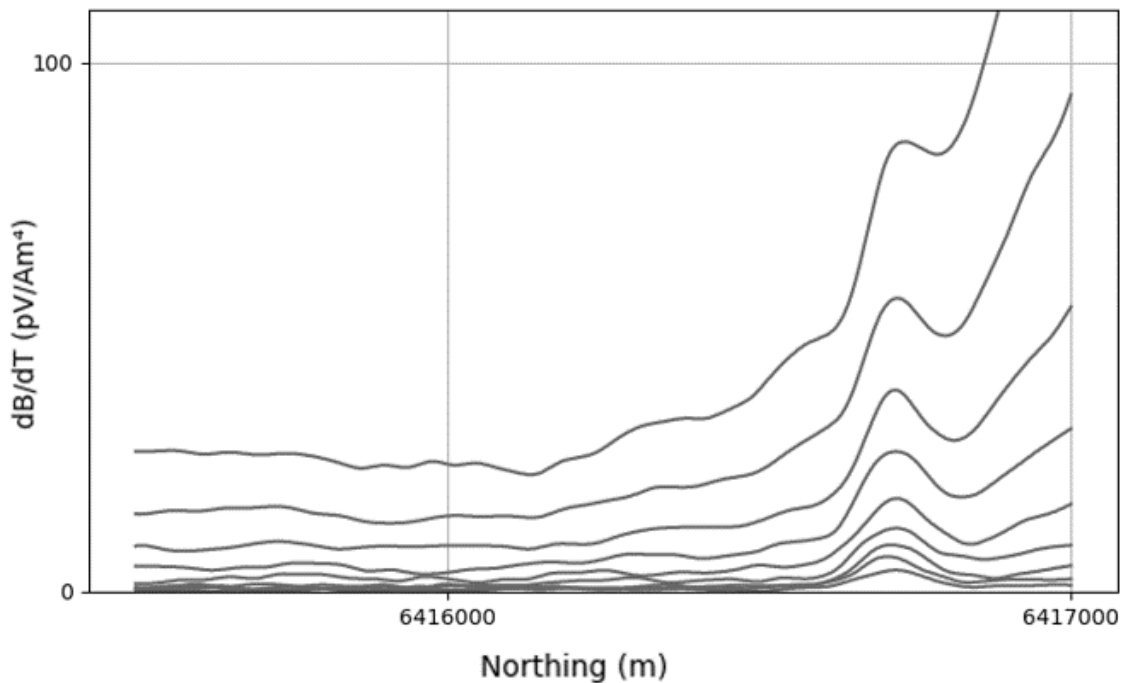


Figure 18: Line 1075 of the HELITEM® data for time windows (21-29) on a linear scale. The flight line passes over the IR2 conductor near 6416700N. Each profile corresponds to a delay time from 2.58 to 11.46 ms after shut off.

Chapter 5

5 Forrestania modelling results

The z-component of the data was chosen to be modelled as it shows the best coupling with the IR2 conductor resulting in the strongest signal-to-noise ratio at the latest time windows. The parameters of the model were manually adjusted in the sphere-overburden program to produce the best fit to the data. The results of the modelling are presented in figure 19, where, the response generated by the program is presented using dashed lines and is overlying the HELITEM® data which is presented using solid lines. In order to show a comparison of the model response with the overburden response on line 1075, the model data has been plotted 300 m on either side of the IR2 conductor. The model parameters for this model are listed in table 2. The body is given a dip of 35 degrees north and is located at a depth of 156 m to the center of the conductor body. The radius of the body was set to 46 m with a conductivity radius squared value (CRS) of 6624 Sm; the overburden is assigned a thickness of 57 m and conductivity of 0.05 S/m. Interpretation of independent EM surveys have estimated a model with a depth of less than 100 m, dipping at approximately 30 – 40 degrees north with a conductance greater than 7000 S (Gilgallon et al, 2019). The parameters of the response generated using the sphere-overburden program are mostly in agreement with the estimates given in Gilgallon et al, (2019), with the exception of a slightly larger depth to target of 156 m in our modelling results and the fact that for a sphere model we estimate a CRS rather than a conductance.

The values used to generate the response were manually tuned to achieve the most accurate fit of the response over the IR2 anomaly, the response generated by the sphere-overburden are non-unique, meaning that there are multiple combinations of model parameters (overburden thickness, overburden conductivity, sphere radius, sphere conductivity) that could produce the same response. The overburden response is larger than the model on the north hand side, but smaller on the south, so the overburden parameters represent a suitable compromise for both sides. Note that the width of the fitted data and measured data are comparable at all delay times.

Forrestania sphere-overburden model parameters	
Depth (m)	156
Strike (degrees)	90
Dip (degrees)	35
Radius (m)	46
Conductivity radius squared (Sm)	6624
Overburden thickness (m)	57
Overburden conductivity (S/m)	0.05

Table 2: Model parameters used in the modelling of the IR2 conductor response at the Forrestania EM test range using the sphere-overburden program.

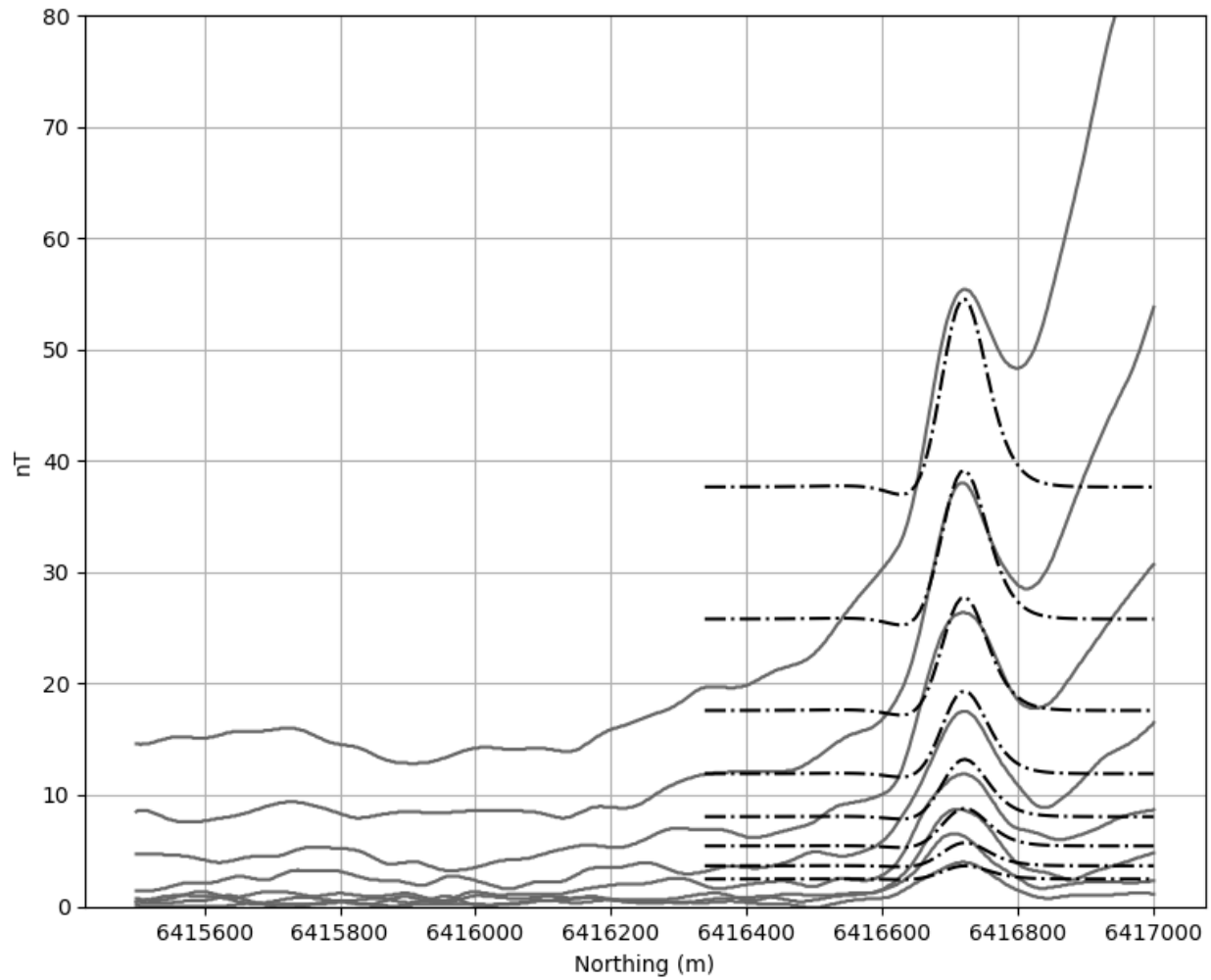


Figure 19: Results of the sphere-overburden modelling (dashed line) overlying the HELITEM® data (solid line) for Line 1075 of the for the late time windows (22-29). The flight line passes over the IR2 conductor at the Forrestania test site.

5.1 Comparison to Maxwell model

The results of the Forrestania models generated using the newly developed sphere-overburden program are compared to published modelling exercises completed on similar data. In Macnae and Hennessy (2019) modelled VTEM Max data over the IR2 conductor. The goal of the modelling in Macnae and Hennessy (2019) was to compare three different modelling algorithms. One of the algorithms used in Macnae and Hennessy (2019) was the Maxwell plate modelling software. The late delay-time windows of the VTEM Max data over a 2.5 km segment of the flight line (black lines) and the Maxwell model result (red lines) are presented in figure 20. Compared with the measured response, the Maxwell model appears too narrow, particularly at the earlier delay times, which is observed in the uppermost profile lines in figure 20 having an increasingly less accurate fit to the VTEM Max data.

The amplitudes are also slightly too large in the earlier windows shown in figure 20, so these aspects of the Maxwell model are not as good as the sphere-overburden model. Further, the Maxwell response on the immediate north and south is too small, whereas the sphere-overburden model was too large to the south and too small to the north. The Maxwell model shows an increase further to the north, perhaps because of a second conductor was placed to the north to try and model the overburden. With further effort it might have been possible to improve the fit to the overburden in the Maxwell model, but modelling multiple bodies can be difficult, particularly if there is inductive interaction. It was concluded by Macnae and Hennessy (2019) that the Maxwell model would be too unstable for use in an inversion algorithm.

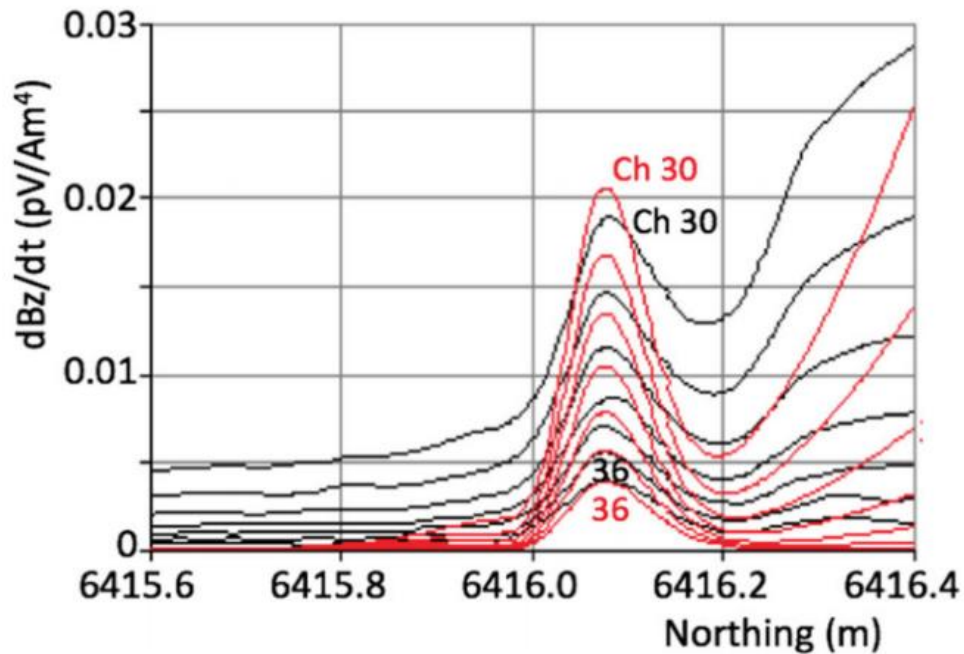


Figure 20: Maxwell model data (red) overlying VTEM Max data (black) from Macnae and Hennessy (2019) from flight line 1075 showing the response of the IR2 conductor at the Forrestania test site.

Both the Maxwell and sphere-overburden models fail to accurately model the response on either side of the IR2 anomaly. In this case, the large variance in overburden thickness and conductivity results in an unsuitable response using both programs. While we presume that the Maxwell model attempts to improve the fit with an extra body to the north, the sphere-overburden program is unable to account for rapid variations in thickness and conductivity of the overburden and is only able to model a constant response for the conductive cover. These results suggest that the sphere-overburden modelling software is capable of achieving a good fit to data in an environment with constant overburden conductance.

Chapter 6

6 Discussion and future work

The sphere-overburden program has been shown to be capable of modelling the airborne EM response of a sphere or dipping plate with optional conductive cover. One limitation is the requirement that the conductive overburden be thin, so if it is too thick, then the early time fit to the data will be poor. The other limitation is if the overburden parameters vary along the profile, the response fit will also be poor. This was evident at Forrestania, where the program was unable to accurately fit the response on either side of the IR2 anomaly.

The software in its current state offers some versatility, ease of use and rapid calculation times. There exists opportunity for future work on the sphere-overburden program to further improve its range of applications and performance. Additional modelling exercises in different geological settings would be useful to further access the programs ability to model airborne EM data in different environments, the Bull Creek deposit in southeast Australia could be a potential deposit for use in a modelling exercise due to the conductive overburden in the area being reasonably representative of that which could be modelled with the sphere-overburden model. Finally, there are some additional options that could feasibly be added to the program to increase its range of uses. For example, 1D inversion along a profile is one such application that could be implemented in the software, another potential feature could be stitched forward models which merge separate sections along a profile to attempt to compensate for the sphere-overburden routines constant overburden assumption. These features if successfully implemented might improve people's ability to use the program for interpretation.

The modelling work done involved exporting the model response and then comparing the field and model data in a separate application. The modelling process could be improved if the field data could be imported into the program and displayed on the same profile as the model data. Another improvement would be to add an inversion algorithm to the package so the program could automatically adjust the model parameters to achieve a good fit. With EM data this normally requires a starting model with a model response reasonably close to the field data.

6.1 Conclusions

We have developed a simple EM forward modelling program that is capable of calculating the EM response of a sphere or dipping-sphere in a resistive host when buried below an overlying thin conductive overburden. The program has distinct advantages over other discrete conductor models such as, ease of use and an efficient run time. Generally, the response calculations are completed in a few seconds after changing parameters. The immediacy of results is of great benefit as a user can specify an orebody of exploration interest and see if the modeled EM response might be observable on a survey. If not, they can change the parameters of the survey (e.g. the base frequency or pulse width) and see if this might result in a stronger more observable response. If it is not possible to detect the target, then the survey might not be worthwhile undertaking. This type of “what if” modelling might also allow the user to determine to what depth orebodies of certain size could be detected below conductive overburden of varying conductance. The program is also of use in an educational setting, it has been successfully incorporated in geophysics classes, where it has proved to be a convenient tool for students to see the change in the decay and shape of the response that might occur when the survey and model parameters are changed.

For example, the students can see how changing the dip and depth and strike orientation changes the EM response. The newly developed sphere-overburden program is consistent with published synthetic examples and able to model real airborne EM data from the Forrestania test site in a manner that is comparable to previously published results. The modelled response directly over the IR2 body is reasonable; however, it has limited ability to model overburdens with variable overburden thickness and conductivity. With further development, additional features and improvements versatility and usefulness could be improved.

References

Dentith, M. C., and Mudge, S. T., 2018, *Geophysics for the mineral exploration geoscientist*: Cambridge University Press.

Desmarais, J. K., and Smith, R. S., 2015a, Survey design to maximize the volume of exploration of the InfiniTEM system when looking for discrete targets: *Journal of Applied Geophysics*, 115, 11–23, DOI: 10.1016/j. jappgeo.2015.02.012.

Desmarais, J.K., and Smith, R. S., 2015b, Decomposing the electromagnetic response of magnetic dipoles to determine the geometric parameters of a dipole conductor: *Exploration Geophysics*, 47, 13–23. <http://dx.doi.org/10.1071/EG14070>

Desmarais, J. K., and Smith, R. S., 2016, Approximate semianalytical solutions for the electromagnetic response of a dipping-sphere interacting with conductive overburden: *Geophysics*, 81(4). DOI: 10.1190/geo2015-0597.1

Dyck, A. V., Bloor, M., and Vallée, M. A., 1980, User manual for programs PLATE and SPHERE: *Research in Applied Geophysics*, 14, University of Toronto Geophysics Laboratory.

Gilgallon, K., Tomlinson, A., and Mortimer, R., 2019, The Forrestania and Nepean electromagnetic test ranges, Western Australia – a comparison of airborne systems: *ASEG Extended Abstracts*, 2019(1), 1–4. DOI: 10.1080/22020586.2019.12073208

Grant, F. S., and West, G. F., 1965, Interpretation theory in applied geophysics. New York: 33 McGraw-Hill.

Hodges, G., Chen, T.-Y. and van Buren, R., 2016, HELITEM® detects the Lalor VMS deposit: *Exploration Geophysics*, 47(4), 285-289, DOI: 10.1071/EG16006

Legault, J. M., Fisk, K., and Fontura, C., 2010, Case study of ZTEM airborne tipper AFMAG results over a magmatic nickel deposit at Forrestania, West Australia, Conference Proceedings, IV Simpósio Brasileiro de Geofísica, Nov 2010, cp-197-00209
DOI: https://doi.org/10.3997/2214-4609-pdb.197.SBGF_2476

Liu, G., and Asten, M. W., 1993, Fast approximate solutions of transient EM response to a target buried beneath a conductive overburden: *Geophysics*, 58, 810–817, DOI: 10.1190/1.1443466.

Prichard, H. M., Fisher, P. C., McDonald, I., Knight, R. D., Sharp, D. R., and Williams, J. P., 2013, The Distribution of PGE and the Role of Arsenic as a Collector of PGE in the Spotted Quoll Nickel Ore Deposit in the Forrestania Greenstone Belt, Western Australia: *Economic Geology*, 108(8), 1903–1921. DOI: 10.2113/econgeo.108.8.1903

Raiche, A., Sugeng, F. and Wilson, G., 2007, Practical 3D EM inversion – the P223F software suite: *ASEG Extended Abstracts*, 1-5, DOI: 10.1071/ASEG2007ab114

Ren, X., Macnae, J., and Hennessy, L., 2019, Three conductivity modelling algorithms and 34 three 3D inversions of the Forrestania test site AEM anomaly: *Exploration Geophysics*, 51(1), 14–24. DOI: 10.1080/08123985.2018.1552072

Slattery, S.R. and Andriashek, L.D., 2012, Overview of airborne-electromagnetic and -magnetic geophysical data collection using the GEOTEM survey north of Calgary, Alberta; Energy Resources Conservation Board, ERCB/AGS Open File Report 2012-09, 168 p.

Smith, R. S., and Lee, T. J., 2001, The impulse-response moments of a conductive sphere in a uniform field, a versatile and efficient electromagnetic model: *Exploration Geophysics*, 32, 113–118, DOI: 10.1071/EG01113.

Smith, R.S. and Salem, A. S., 2007, A discrete conductor transformation of airborne electromagnetic data: *Near Surface Geophysics*, 5, 87-95. <https://doi.org/10.3997/1873-0604.2006021>

Smith, R.S., and Wasylechko, R., 2012, Sensitivity cross-sections in airborne electromagnetic methods using discrete conductors: *Exploration Geophysics*, 43, 95-103. <https://doi.org/10.1071/EG11048>

Sørensen, K. I., and Auken, E., 2003, SkyTEM - new development in high-resolution airborne TEM: 9th EAGE/EEGS Meeting. DOI: 10.3997/2214-4609.201414517

Telford, W. M., Geldart, L. P., and Sheriff, R. E., 1990, *Applied Geophysics*. DOI: 10.1017/cbo9781139167932

Vallée, M. A., 2015, New developments in AEM discrete conductor modelling and inversion: 35
Exploration Geophysics, 46, 97–111, DOI: 10.1071/ EG14025.

Huebener, R. (2014). Conductors, semiconductors, superconductors. Heidelberg: Springer.